Immunobiology 225 (2020) 151874

Contents lists available at ScienceDirect

Immunobiology

journal homepage: www.elsevier.com/locate/imbio

Regulation of hepcidin/iron-signalling pathway interactions by commensal bifidobacteria plays an important role for the inhibition of metaflammation-related biomarkers

Darab Ghadimi[a,*], Mohamed Farghaly Yoness Hassan[a,1], Regina Fölster-Holst[b], Christoph Röcken[c], Michael Ebsen[d], Michael de Vrese[a], Knut J. Heller[a]

[a] Department of Microbiology and Biotechnology, Max Rubner-Institut, Hermann-Weigmann-Str 1, D-24103, Kiel, Germany
[b] Clinic of Dermatology, University Hospital Schleswig-Holstein, Schittenhelmstr. 7, D-24105 Kiel, Germany
[c] Institute of Pathology, Kiel University, University Hospital, Schleswig-Holstein, Arnold-Heller-Straße 3/14, D-24105, Kiel, Germany
[d] Städtisches MVZ Kiel GmbH (Kiel City Hospital), Department of Pathology, Chemnitzstr.33, 24116, Kiel, Germany

ARTICLE INFO

Keywords:
Metaflammation
Bifidobacteria
Iron
Hepcidin
IL-6

ABSTRACT

Increased concentration of ferrous iron in the gastrointestinal tract increases the number of various pathogens and induces inflammation. LPS and/or high-fat diet-associated metaflammation is mediated through a quaternary receptor signaling complex containing iron-regulated pathway, IL-6/STAT inflammatory signaling pathway, hepcidin regulatory pathway, and common TLR4/NF-κB signaling pathway. We, therefore, investigated whether bifidobacteria directly or indirectly ameliorate LPS- and/or high-fat diet-associated metaflammation by reduction of intestinal iron concentration and/or the above-mentioned pathways.

Material & methods: We used a triple co-culture model of HT-29/B6, HMDM and HepG2 cells with apically added *Bifidobacterium pseudolongum* (DSMZ 20099), in the absence or presence of iron, LPS or oleate. Expressions of the biomarkers of interest were determined after 24 h incubation by TaqMan qRT-PCR, cell-based ELISA or Western blot.

Results: Bifidobacteria inhibited LPS- and oleate-induced protein expression of inflammatory cytokines (IL-6, TNF-α) concomitantly with decreases in cellular TG and iron concentration. Exposure of co-cultured cells to bifidobacteria blocked NF-kB activity through inhibition of IκBα, p38 MAPK, and phosphorylation of NF-kB 65 subunit. TaqMan qRT-PCR and Western blot analysis revealed that bifidobacteria downregulated mRNA and protein expression of BMP6, DMT1, hepcidin, L-ferritin, ferroportin, IL-6, TfR1, Stat3, and TLR4 following exposure to excessive extracellular LPS, oleate and iron. However, the patterns of TLR2 mRNA and protein expression were quite the opposite of those of TLR4.

Conclusion: Commensal bifidobacteria ameliorate metaflammation/inflammatory responses to excessive extracellular LPS, oleate and iron through at least two molecular/signaling mechanisms: i. modulation of interactions of the hepcidin- and iron-signaling pathways via reduction of excess iron; ii. reduction of pro-inflammatory cytokines and hepcidin production through inhibition of the TLR4/NF-kB pathway. This may be a molecular

Abbreviations: BMP6, bone morphogenetic protein 6; BSA, bovine serum albumin; *B.p*, *Bifidobacterium pseudolongum*; *B.t*, *Bifidobacterium thermophilum*; CFS, cell-free culture supernatants; CFU, colony forming units; ddH2O, double-distilled water; DMEM/F-12, Dulbecco's modified eagle medium/nutrient mixture F-12; DIOS, dysmetabolic iron overload syndrome; DMSO, dimethyl sulfoxide; DMT1, divalent metal transporter 1; ELISA, enzyme-linked immunosorbent assay; EPEC, enteropathogenic *Escherichia coli*; EU, endotoxin units; FPN1, ferroportin 1; FTL1, ferritin light chain subunit; GAPDH, glycerol aldehydephosphate dehydrgenase; HAMP, hepcidin-encoding gene; HFD, high-fat diet; HMDM, human monocyte-derived macrophage; IκBα, nuclear factor of kappa light polypeptide gene enhancer in B-cells inhibitor, alpha; IRP1, iron regulated protein-1; LAB, lactic acid bacteria; L-ferritin, low chain ferritin; IL-1β, interleukin-1β; IL-6, interleukin-6; IL-6R, interleukin-6 receptor; JNK, c-Jun N-terminal kinase; LPS, lipopolysaccharide; MAMPs, microbe-associated molecular patterns; MOI, multiplicity of infection; MTT, 3-(4, 5 - dimethyl-thiazol-2-yl)-2,5-diphenyltetrazoliumbromide; NAFLD, non-alcoholic fatty liver disease; NASH, non-alcoholic steatohepatitis; NF-kB, nuclear factor 'kappa-light-chain-enhancer' of activated B-cells; p38 MAPK, p38 mitogen activated proteinkinases; PBS, phosphate buffer saline; PVDF, polyvinylidene difluoride; qRT-PCR, quantitative reverse transcription polymerase chain reaction; SEM, standard error of the mean; STAT3, signal transducer and activator of transcription 3; TEER, transepithelial/transendothelial electrical resistance; TfR1, transferrin receptors protein 1; TG, triglycerides; WB, Western blotting

* Corresponding author at: Department of Microbiology and Biotechnology, Max Rubner-Institute, Hermann-Weigmann-Straße 1, 24103, Kiel, Germany.
E-mail address: darab.ghadimi@mri.bund.de (D. Ghadimi).
[1] Present address: Dairying Department, College of Agriculture, Sohag University, Sohag, Egypt.

https://doi.org/10.1016/j.imbio.2019.11.009
Received 12 July 2019; Received in revised form 20 November 2019; Accepted 25 November 2019
Available online 29 November 2019

basis by which commensal bifidobacteria enhance intrinsic cellular tolerance against excess consumption of energy-yielding substrates and/or free iron.

1. Introduction

Previous studies have shown that, on one hand, increased availability of iron in the gastrointestinal tract directly affects the gut microbiota composition by reducing the numbers of the beneficial microbiota (e.g., bifidobacteria) and the spreading of pathobionts. On the other hand, excess available iron may indirectly affect host–microbe interactions and cellular lipid metabolism via induced inflammation (Ahmed et al., 2012; Kell and Pretorius, 2015; Li and Frei, 2009; Yilmaz and Li, 2018). The precise molecular basis and biochemical causes are not well understood.

The nutrient essential for almost all bacteria, except for lactic acid bacteria (LAB), is iron (Bailey et al., 2011). LAB do not need iron in their natural environment, which may be a crucial advantage over other microorganisms. For instance, *Lactobacillus delbrueckii* affects the function of other microbes by binding iron hydroxide to its cellular surface, thus making it unavailable to other microbes (Markowiak and Śliżewska, 2017).

Bifidobacteria and LAB have been shown to remove soluble ferrous iron from media and from their environment by internalizing it and - when oxygen is present - partially oxidizing it to insoluble $Fe(OH)_2$ by putative intracellular ferroxidases (Kot et al., 1995). The ability of bifidobacteria to efficiently sequester iron in the gut is a mechanism of competition for nutrients, causing iron starvation in EPEC bacteria (Vazquez-Gutierrez et al., 2015). It has been also shown hat: (i) efficient competition for iron is a key factor for bacterial growth, persistence and establishment in the intestine; and (ii) the iron-related inflammatory diseases also have a major microbial component involving the resuscitation of dormant organisms and their shedding of inflammatory molecules, especially of cell wall components such as LPS (Kell and Pretorius, 2015; Vazquez-Gutierrez et al., 2016).

It is also well known that elevated levels of extracellular iron may result in increased gastrointestinal tract pathogen toxicity, resulting in increased intestinal permeability and inflammation. The normal microbiota is unable to thrive in an environment high in iron, because it is 'out-competed' by the bacterial overgrowth of pathogenic bacteria. This 'out-competition' leads to increased intestinal inflammation and subsequently to intestinal permeability, which may in turn allow pathogens to reach the liver where they can initiate inflammation and NAFLD. Restoring the gastrointestinal tract environment may allow the natural gastrointestinal tract microbiome to prosper and restrict the growth of pathogenic bacteria (Briskey, 2015).

The liver is: (i) an important site for iron and lipid metabolism; (ii) the main site for the initial phase of removal of LPS and Gram-negative bacteria from the bloodstream; and (iii) the main site for the interactions between these metabolic pathways (Ahmed et al., 2012; Gregor and Hotamisligil, 2011; Kell and Pretorius, 2015). One role of iron in the pathogenesis of diseases associated with hyperlipidemia and lipid deposition is likely to include an ability to induce oxidative stress and inflammation in the liver. Lipoprotein uptake pathways are affected by iron. In vitro studies in HepG2 cells showed that iron overload increases intracellular lipid droplet formation. Furthermore, iron accumulation has a pro-inflammatory and pro-fibrogenic role by activating Kupffer cells to release inflammatory cytokines (Ahmed et al., 2012).

Regarding cross-linking between lipid and iron metabolism, high-fat diet (HFD) was associated with increased expression of the major iron uptake protein transferrin receptor-1 (TfR-1) and with upregulation of the intracellular iron sensor iron regulated protein-1 (IRP1). Supplementation with fatty acids induced TfR-1 and IRP1 in HepG2 hepatocytes, favoring intracellular iron accumulation upon exposure to iron salts (Dongiovanni et al., 2015; Meli et al., 2013).

Iron metabolism/levels is/are tightly controlled by regulatory mechanisms that integrate both local and systemic signals under both normal and high iron conditions. Local signaling is mediated by iron regulatory proteins (IRP1 and IRP2) (Scheers and Sandberg, 2014), which bind to iron response elements (IRE) in the mRNAs encoding factors associated with iron metabolism. In addition to IRP-mediated regulation of cellular iron levels, iron metabolism is regulated systemically, which is achieved by hepcidin synthesis/secretion regulatory mechanism (Cassat and Skaar, 2013). Hepcidin, a peptide hormone with antimicrobial activity predominantly expressed in the liver, plays an essential role in maintaining normal iron homeostasis (Wang et al., 2008). It regulates post-translationally ferroportin and thus controls entry of iron into the plasma after absorption to enterocyte. Increases in total body iron stores trigger the production of hepcidin, which subsequently induces the internalization and degradation of ferroportin. As ferroportin is present on the surfaces of macrophages, hepcidin also decreases iron export after recycling by the reticuloendothelial system. Synthesis and secretion of hepcidin by the liver is controlled by iron stores within macrophages, inflammation, hypoxia, and erythropoiesis. Macrophages communicate with the hepatocytes to regulate hepcidin release into the circulation via different proteins such as BMP6 and transferrin. Inappropriate production of hepcidin contributes to the pathogenesis of various iron disorders. Hepcidin deficiency results in the development of systemic iron overload because of excessive iron absorption, whereas relative excess of hepcidin causes iron restriction and anemia (Nemeth 2009). Hepcidin release from the liver is also stimulated by pro-inflammatory cytokines and TLR4 activation. In addition to hepcidin production in the liver, macrophages synthesize hepcidin in response to infectious agents, allowing for modulation of iron availability at the infectious focus (Cassat and Skaar, 2013).

The relationship between low-grade inflammation, metabolically triggered inflammation described as "metaflammation" (Dixit, 2008), and iron status is well described (Ahmed et al., 2012; Aravindhan and Madhumitha, 2016; Bailey et al., 2011; Fabersani et al., 2017; Li et al., 2018; Moen et al., 2018; Mraz and Haluzik, 2014). This aspect of inflammation - "low grade" or metaflammation - is due to the dysfunction of the immune system: at optimal level it confers protection against pathogens; at the suboptimal level it leads to immunodeficiency; and at supraoptimal level it leads to inflammation (Aravindhan and Madhumitha, 2016; Fabersani et al., 2017). However, previous studies have shown the existence of a highly responsive LPS – iron - IL-6-hepcidin axis linking innate immunity, iron metabolism (Kemna et al., 2005), and association of dysregulation of NF-κB, MAPK, or JAK-STAT activity with inflammatory and metabolic diseases (Chen et al., 2017; McNelis and Olefsky, 2014; Aravindhan and Madhumitha, 2016; Li et al., 2018).

These data suggest that LPS, excess iron and/or high-fat diet-associated metaflammation are mediated through a quaternary receptor signaling complex containing iron-regulated pathway, IL-6/STAT inflammatory signaling pathway, hepcidin regulatory pathway, and common TLR4/NF-κB signaling pathway.

Despite these excellent data and although many studies have focused on the beneficial metabolic effects of commensal bifidobacteria and on the metabolic fate of an oral iron load, few (or no) have emphasized the LPS/iron/hepcidin – IL-6/STAT - TLR4/NF-kB - p8 MAPK quaternary receptor signaling complex pathway. We, therefore, investigated the possible role of downstream signaling in the modulation of cellular lipid metabolism by *Bifidobacterium pseudolongum* and *Bifidobacterium thermophilum* in presence or absence of LPS, iron, or

oleate, using a triple co-culture models consisting of enterocytes, hepatocytes and macrophages and propose a new mechanism describing the role of commensal bifidobacteria on the inhibition of metaflammation in response to excess nutrients (e.g., Iiron), energy, (oleate), and LPS.

2. Material & methods

2.1. Materials, reagents, solutions, antibodies, and kits

Antibodies against the following proteins were purchased from Cell Signaling Technology (Leiden, The Netherlands): phospho-JNK (pJNK, Thr183/Tyr185), JNK, phospho-NF-κB p65 (p-NF-κB p65, Ser536), NF-κB p65, IκBα, phospho-p38 MAPK (Thr180/Tyr182), p38 MAPK, phospho-STAT3, STAT3.

A polyclonal rabbit anti-hepcidin 25 (ab30760) and primary antibodies to DMT1 and TfR were purchased from Abcam (Berlin, Germany). Actin and GAPDH antibodies were from Sigma-Aldrich (Taufkirchen, Germany). Human IL-6 antibody (no. MAB206-100) was purchased from R&D Systems (Bio-Techne GmbH, Wiesbaden, Germany). All other antibodies, including horse-radish peroxidase-COnjugated secondary antibodies (mouse and rabbit) were purchased from Santa Cruz Biotechnology, Inc. (Heidelberg, Germany). IL-1β and IL-6 ELISA kits were purchased from BD Biosciences (Heidelberg, Germany). Cell-based ELISA kit for measuring cellular triglycerides was purchased from Cayman Chemical (Biomol GmbH, Hamburg, Germany). Human hepcidin ELISA kit for measuring hepcidin concentrations in cell-free supernatants were purchased from BioCat (Heidelberg, Germany). TransAM NFκB colorimetric kits for measuring NF-kB DNA binding activity was purchased from Active Motif Europe (La Hulpe, Belgium). Ultra-pure LPS (E. coli 026:B6), Corning Transwell®-COL inserts (Cat# CLS3493, Corning, 12-well, 0.4 μm, 12 mm), ferric citrate (F3388), sodium oleate (O-7501), and fatty acid-free bovine serum albumin (BSA) were all purchased from Sigma-Aldrich Chemie GmbH (Taufkirchen, Germany). DMEM/F-12 medium was purchased from Fisher Scientific GmbH (Schwerte, Germany).

Stock solutions containing oleate were prepared by dissolving the fatty acid in 50 % ethanol to a final concentration of 100 mM. The stock solutions were then diluted to a final concentration of 1 mM oleate in DMEM/F-12 culture medium containing 0.5 % fatty acid-free BSA. This working solution was always freshly prepared and sterilized by filtration through a 0.22-μm syringe filter.

Ferric citrate was dissolved in sterile deionized water by gentle agitation and heating at 65 °C, followed by sterilization using a 0.22-μm (bacterial retentive) filter and storage at 4 °C. A working solution of 100 μM ferric citrate was always freshly prepared by dilution in DMEM/F-12 culture medium. Cell cultures were exposed to the fatty acid or iron for 24 h at which point the cell confluence was 70–80 %.

2.2. Bacterial strains and growth conditions

Species of bifidobacteria that have been characterized as iron-utilizing (Kot et al., 1995) were used. These were: *Bifidobacterium pseudolongum* (*B. pseudolongum*, DSMZ 20099 = ATCC 25526) and *Bifidobacterium thermophilum* (*B. thermophilum*, DSMZ 20212 or ATCC 25866). Bacterial strains were propagated as previously described (Ghadimi et al., 2011). Briefly, using a 0.02 % inoculum from stocks stored at −80 °C in 30 % glycerol, bacteria were grown anaerobically (The Modular Atmosphere Controlled System, MACS-VA500 workstation with airlock; Don Whitley Scientific Limited, Bingley, UK) in MRS broth medium (Lactobacilli MRS according to de Man, Rogosa, Sharpe; Merck, Darmstadt, Germany), at 37 °C for 12 h. Colony forming units (CFU) per ml of each bacterial culture were estimated as previously described (Ghadimia et al., 2018). The bacterial cultures were centrifuged at 4 °C at 5000 × *g* for 10 min. After washing three times with endotoxin-free phosphate-buffered saline without Ca^{2+} and Mg^{2+} (DPBS; BioWhittaker, Lonza, Basel, Switzerland), the bacterial pellet was suspended to 2×10^7 CFU in 50 μL of cell culture medium (see below). This prepared suspension was added to cultures of HT-29/B6 cells to give bacteria-to-cell ratios of 10:1. Dilutions were also plated on agar plates. After 48 h of incubation, colonies were counted to confirm the accuracy of dilution and viability of bacteria.

As an established Gram-negative model organism, some preliminary experiments were conducted with live, dead and cell-free culture supernatants (CFS) of *E. coli* laboratory TG1 strain (DSM No.: 6056, K12 TG1 or Cat# BU-00035, Maxim Biothec Inc, CA, USA), rtespectively. The TG1 strain was grown at 37 °C in Luria broth. *E. coli* K12, harvested from aerobic, anaerobic, or oxygen-limited cultures, reduces Fe (III) citrate, converting it to soluble Fe (II), which is the transportable/absorbable form of iron for intestinal absorptive cells [Cassat and Skaar, 2013; Williams and Poole, 1987]. For experiments with heat-killed *bacteria,* the liquid cultures were heated to 95 °C for 30 min. To verify that heat-treatment had successfully killed the bacteria, undiluted bacterial suspensions were plated on appropriate agar plates. Only suspensions not yielding colony-formation were used in the experiments. However, a set of separate preliminary experiments were also conducted with CFSs to elucidate whether CFS had immunomodulatory effects in co-cultured cells. The supernatants were recovered by centrifugation at 12000 rpm and 40 °C in an Eppendorf 5810 R (Eppendorf) centrifuge for 10 min. CFSs were carefully removed, neutralized to pH 7.0 by the addition of 1 N NaOH, and concentrated ten-fold by lyophilization. The resulting supernatants were sterilized by passing through 0.22-μm pore size sterile and pyrogen-free filters (Sarstedt, Nümbrecht, Germany). Aliquots of CFS samples were stored at −80 °C until use. Viability assays were conducted after storage to exclude contaminations or presence of viable cells. Fresh aliquots of samples were thawed for every new experiment to minimize variations in the samples between experiments. The supernatants were added to the co-culture medium at concentrations of 7 % v/v (Bermudez-Brito et al., 2013).

Endotoxins affect both *in vitro* and *in vivo* cell growth and function (particularly stimulate IL-6 production) and are a source of significant variability. Hence, the presence of LPS in the assays was determined in the bifidobacteria cultures by a limulus amebocyte lysate assay (BioWhittaker, Walkersville, MD). The LPS concentration in the experiments with 10:1 bacterium–to-cell ratio was found to be less than 0.5 EU/mL.

2.3. Cell cultures and experimental model

We used a traditional three different cell types-based triple co-culture model, according to previously published procedures (Ghadimia et al., 2018), in which polarized enterocytes (iron-absorbing cells), hepatocytes (metabolizing cells), and macrophages (immune cells) were assembled together to closely mimic the physiological *in vivo* situation, where hepatocytes interact with other cell types through soluble signalling factors. This co-cell culture models consisted of polarized HT-29/B6 and/or T84 cells, HepG2 and/or Hu7h cells, and HMDMs. to provide an opportunity for the co-culture of multiple types of cells to mimic the *in vivo* conditions, where macrophages secrete cytokines, such as IL-6, which in turn stimulate the liver to secrete - among others - hepcidin. Also, in this model the metabolite pattern *in vivo* in an inflammatory milieu and under excess available iron are more adequately represented.

To assure only TLR4-mediated signaling, cells were treated with ultrapure LPS. The cell cultures were periodically assessed for presence of mycoplasma as described before (Ghadimia et al., 2018). The cell cultures were always found to be free of any contamination.

2.3.1. Preparation of pure monoculture traditional 2D polarized enterocytes

A polarized monolayer of intestinal epithelial HT-29/B6 cells and /or T84 cells with both apical (AP) and basolateral (BL) compartments

was stabilized as previously described (Ghadimi et al., 2010). Briefly, HT-29/B6 and/or T84 cells (1×10^5 cells per cm^2) were grown in Transwell®-COL inserts separating AP and BL compartments. To qualitatively determine confluence and formation of tight junctions of T84 cells, the TEER across the monolayer was monitored as previously described (Ghadimi et al., 2009). T84 cells were utilized for experiments after 3 weeks, when the confluent monolayers had formed. Only intact polarized cell monolayers exhibiting a net resistance of > 1000 Ω × cm^2 were used. The polarized HT-29/B6 cells seeded on the AP surface of the Transwell ®-COL membrane inserts, were maintained in a humidified 37 °C incubator with 5 % CO_2 water saturated atmosphere for 14 days to allow for full differentiation of the cells. The medium was changed every second or third day and the cells were passaged at approximately 80 % confluence. Stock cultures of HT-29/B6 and/or T84 cells were maintained in DMEM F-12 medium.

2.3.2. Preparation of pure monoculture traditional hepatocytes

Traditional 2D hepatocytes, human hepatoma cell lines HepG2, and/or Huh7 (our laboratory stocks, ATCC/LGC, Wesel, Germany) were grown under standard conditions as previously described (Ghadimia et al., 2018). Briefly, HepG2 and/ or Huh7 cells at passage 62–65 were seeded at the bottom of 12-well Transwell®-COL inserts (Cat# CLS3493, Corning, 12- well, 0.4 µm, 12 mm) at 200,000 cells/well. Stock cultures of HepG2 and/or Huh7 cells were maintained in minimal essential medium (MEM) with Earle's salt. We used two well-studied hepatic cell lines, namely HepG2 and Hu7h cells, since constituting only one type of human hepatocellular carcinoma cell line, cannot be regarded as being representative of the primary hepatocytes. However, in all subsequent experiments, we preferentially used HepG2 cells since they have been employed extensively in the screening of LPS- and cytokine-induced effects on lipid metabolism (Ghadimia et al., 2018), and they appear to be a very suitable model for studying energy-dependent regulation of the cellular iron metabolism and antioxidative effects of lactic acid-producing bacteria (Ghadimia et al., 2018; Kitaura et al., 2015; Scheers et al., 2016).

2.3.3. Preparation of pure monoculture macrophages

Human monocyte-derived macrophages (HMDMs) were prepared according to previously published procedures (Ghadimi et al., 2008, 2010, 2018, 2019).

2.3.4. 2D enterocytes-2D macrophages-2D hepatocytes triple cell co-culture model

The triple cell co-cultivation models were set up as previously described (Ghadimi et al., 2019) and as shown in Fig. 1 A–D. Direct contact between HMDMs and HT-29/B6 was achieved through the 0.4 µm pores of the membrane, while, in the case of HepG2 cells, only bacteria-secreted factors could freely diffuse in the culture medium and through the pores to reach the HepG2 cells. The combined cell lines (done in triplicates) were allowed to equilibrate for another 24 h before the experiments. *B. pseudolongum* and *B. thermophilum* (bacteria to cell ratio of 10:1) in antibiotic-free DMEM-F-12 were added to the upper reservoir of Transwell®-inserts containing confluent polarized HT-29/B6 and/or T84 monolayers in the presence and absence of either excess iron (100 µmol/L of ferric citrate) (Li and Frei, 2009) and oleate (1 mM) or LPS (100 ng/ml), which was applied to the BL sides of the polarized HT-29/B6 and/or T84 monolayers. The AP medium in all plates was exchanged for freshly prepared DMEM-F-12, non-supplemented or supplemented with iron. Iron concentration in AP chambers was 100 µmol/L. Addition of LPS and measuring of TEER was done as described previously (Ghadimi et al., 2019). Based on dose and time-course experiments, HT-29/B6 monolayers were consistently considered in most of the experiments and their effects are preferably shown in this study.

The bacterial pellet was diluted to 1×10^7 CFU in 50 µl of appropriate cell culture medium and was freshly added to cell cultures to

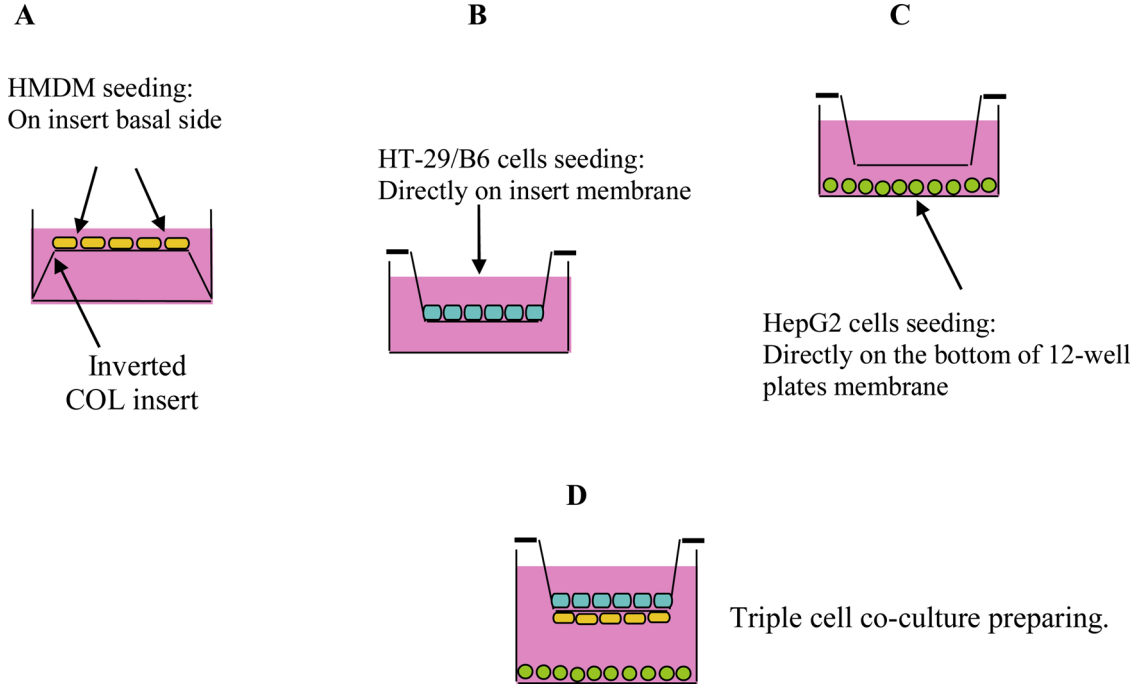

Fig. 1. Schematic illustration of the three different cell type-based cell co-culture model showing experimental setup in the *in vivo*-mimicking trans-well system for assessment of high-iron diet/LPS/oleate–mediated metaflammation and disrupted cellular energy metabolism. (**A- D**) Schematic drawing of the preparation of the in vitro traditional triple cell co-culture model with HT-29/B6 and/or T84 cells, HMDMs and HepG2 cell mimicking the human intestine-liver inter-organ interactions. In the beginning of culture period, the inserts were inverted with basal sides facing upwards and placed in a deep glass dish. HMDM cells were seeded onto the basal sides at concentration of 5000 HMDM/insert (Ghadimi et al., 2010, 2018, 2019) (**A**). After three days of incubation, the HMDM were assumed to attach to the basal sides of the inserts and the inserts were inverted to their original orientation. For the triple cell co-cultures setup, 5000 HT-29/B6 cells were seeded into inserts' apical sides (**B**). 12-well plates were seeded with HepG2 cells (**C**). Inserts were placed into the wells of 12-well plates (**D**).

yield a bacteria-to-cell ratio of 10:1, which is a biologically relevant dose of bacteria (Ghadimia et al., 2018).

The most commonly used doses of stimulators/inhibitors were chosen based on manufacturer's protocols, our own preliminary experiments, or previous studies. For example, the concentration of oleate, 1 mM, was used as previously described (Ghadimia et al., 2018). It has been shown that oleate had no cytotoxic effects at this concentration, but induced lipid accumulation in different cell types like HepG2 cell (Kitaura et al., 2015). Stock fatty acid solution (100 mM) in DMSO was prepared and added to the media as described previously by Kitaura et al. (2015).

Ferric citrate, was used because (i) the majority of labile iron in humans is found as a complex of ferric iron with citrate (Li and Frei, 2009), (ii) the toxicological effects of Fe (II) on enterocytes are higher than those of Fe (III=), (iii) at comparable concentrations, Fe (II) can cause higher LDH release values than Fe (III) (He et al., 2008).

After incubation, cell-free supernatants were collected from both compartments (AP and luminal cell milieu of co-cultured cells) and sterilized using 0.22 μM filters. These cell- and bacteria-free supernatants were then used for measuring absorption of iron by the cells (enterocytes) and levels of hepcidin, L-ferritin, IL-1β and IL-6. Iron absorption by the cells and ferritin light chain were assessed enzymatically with an automatic Konelab™ 20 Clinical Chemistry Analyzer (Thermo Fisher Scientific Inc., Waltham, MA, USA), loading a drop of supernatant instead of serum. The levels of hepcidin, released into the luminal cell milieu of co-cultured cells, were measured using Human Hepcidin Quantikine ELISA Kit (R&D Systems (Bio-Techne GmbH, Wiesbaden, Germany). IL-1β and IL-6 were quantified by commercial ELISA kits were from BD Biosciences (Heidelberg, Germany). Cell lysates were used for direct determination of cellular triglycerides by cell-based ELISA Kit (BioCat, Heidelberg, Germany).

The effect of bacteria, iron, LPS, and oleate on cell viability was determined by MTT assay. After harvesting culture supernatants and recording TEER measurements, the assay medium was discarded from the top well and Transwell® inserts were transferred to a new empty 24-well plate. The conversion of water soluble MTT to an insoluble formazan for each cell type was determined using *in vitro* Toxicology Assay Kit, MTT based (Sigma-Aldrich (Taufkirchen, Germany).

2.4. Molecular assessments

2.4.1. TaqMan real-time quantitative polymerase chain reaction (TaqMan RT-qPCR)

Cellular RNA from HT-29/B6, HMDMs and HepG2 cells was purified using the RNeasy® Mini Kit (Qiagen Gmbh, Hilden, Germany) according to the manufacturer's instructions. Genomic DNA was removed by using the RNase-Free DNase Set (Qiagen cat. no. 79254), according to the manufacturer's manual. Quality and quantity of RNA samples were assessed as previously described (Ghadimi et al., 2009). Samples were stored at −80 °C.

1 μg RNA was transcribed to cDNA using TaqMan reverse transcription reagents. qRT-PCR was performed in 50-μl volumes for the indicated genes containing 25 μl TaqMan® universal PCR Master Mix with AmpliTaq Gold polymerase, 22.5 μl TaqMan® assays–on-demand primer/probe mixture (BMP6: Hs01099594_m1; DMT1: Hs00205888_m1; L-ferritin: Hs00830226_gH; ferroportin: Hs00205888_m1; GAPDH: Hs99999903_m1; HAMP: Hs00221783_m1; IL-6: Hs00174131_m1; STAT3: Hs01047579_m1; TfR1: Hs00951083_m1; TLR2: Hs01872448_s1; TLR4: Hs00152939_m1), and 2.5 μl sterile ddH2O containing cDNA corresponding to 10 − 20 ng RNA (depending on the target gene). Reactions were run on an ABI PRISM 7000 Sequence Detection System (all reagents were purchased from Applied Biosystems, Darmstadt, Germany). The results were analyzed with the SDS software package version 2.1. qRT-PCR assays were performed in at least three independent experiments. Besides the cDNA sample, each TaqMan assay included a fixed standard and a no-template control. The data for each sample were normalized to the GAPDH mRNA level present in each sample, normalized again between the samples to the levels of the indicated mRNA present in the control, and then relative expression levels were determined. Two further negative controls (no RNA, no RT), in which RNA and RT product were replaced by water during the RNA preparation and cDNA synthesis step, were included to exclude any DNA contamination in RNA preparations and cDNA synthesis step. Lack of DNA contamination in the PCR amplification step was verified by failure of PCR to produce any amplicon in the absence of a cDNA template.

2.4.2. SDS-PAGE and Western blot (WB) analysis

Following removal of culture medium, cell monolayers were first washed twice in sterile PBS. HT-29/B6, HMDM and HepG2 cells were then harvested using a cell scraper. Crude membrane extracts were prepared as described (Ghadimi et al., 2009 and 2018 WB analysis was carried out as previously described (Ghadimi et al., 2009 and 2018). Briefly, cells were lysed in ice-cold lysis buffer containing 50 mM Tris-HCl, pH 8.0, 150 mM NaCl, 1 % Nonidet P-40, 0.5 % deoxycholate, 0.1 % SDS, 1 mM phenylmethyl sulfonyl fluoride, and 150 units/ml of aprotinin. After centrifugation, protein samples were separated by SDS-PAGE gel electrophoresis in running buffer, washed in Tris-buffered saline with Tween-20, transferred to a nitrocellulose or PVDF membrane and were analyzed by immunoblotting. Following successful transfer, membranes were probed using antibodies specific to the target proteins to assess the protein expression of total IL-6, total p38 MAPK, phospho- p38 MAPK, IκBα and phospho- NF-κB p65 subunit (both as nuclear translocation of NF-kB). Primary antibodies targeting IκBα (1:1000), IL-6 (1:200), p-NF-κB p65 (1:1000), p-p38 MAPK (1:1000), DMT1 (1:1000), hepcidin-25 (1:100), p-JNK (1:1000), p- STAT3 (1:1000) and TfR1 (1:1000) as well as secondary antibody conjugated with horseradish peroxidase (HRP) (1:10,000) were used for protein quantification. Detection of β-actin (Sigma-Aldrich (Taufkirchen, Germany, 1:10,000 antibody dilutions) was used as control for equal loading of protein. Blots were developed with enhanced chemiluminescent (ECL) (Amersham Pharmacia Biotech). Band intensities were quantified by 2D-scanning using a Hirschmann Elscript 400 densitometer and the program SCAN 400 (Hirschmann, Unterhaching, Germany).

2.4.3. NF-kB DNA binding activity assay

ELISA-based TransAM NF-κB colorimetric Kit (Active Motif Europe, La Hulpe, Belgium) was applied according to the manufacturer's instructions. Bifidobacteria were added to the apical compartment in the presence of 100 μmol iron in the AP chamber, 100 ng LPS/ml in the BL chamber, and 1 μmol oleate in the both AP and BL chambers. After incubation for 24 h, whole-cell extracts from HepG2 (as liver cell model and systemic target cells for bifidobacteria-secreted factors) were assayed for overall NF-κB p65 activity, by using the TransAM NF-κB p65 transcription factor assay kit, and NF-κB luciferase reporter assay as indicated below.

2.4.4. Transfection and NF-κB-dependent promoter luciferase reporter gene assays

NF-kB promoter activity was determined as described previously (Ghadimia et al., 2018 and 2019).

2.5. Statistical analysis

STATGRAPHICS Plus statistical software-Version 4.1 was applied for statistical analysis. Data were treated by analysis of variance (ANOVA). Because of a non-normal distribution of most of the data, nonparametric Mann-Whitney *U* test was used to compare cytokine data. This test allowed comparing data from cultures in the absence of a bacterial strain with cultures in the presence of different strains. In the case of cytokines data, all experimental data were expressed as the

mean ± SEM and were considered statistically significant when $p < 0.05$.

3. Results

In this presentation, we consistently considered the effects of live *B. pseudolongum,* although *B. thermophilum* and dead *B. pseudolongum* were also examined. The reasons for this were: i) *B. pseudolongum* modifies colonic microbiota and increases mucus layer thickness *in vivo* (Mangin et al., 2018); and ii) in our experiment and after 24 h incubation, TEER values in live *B. pseudolongum* group were found to have the highest levels.

3.1. Cell viability and cytotoxicity assay

The effects of bacteria, iron, LPS, and oleate on cell viability were determined by MTT reduction assay. Total viable and nonviable cells were counted by trypan blue exclusion and inclusion using a hematocytometer as described previously (Ghadimi et al., 2010). All of the components tested above and under these assay conditions, had no statistically significant effect on overall cell viability (data not shown).

3.2. Transepithelial electrical resistance values across the monolayer of polarized human enterocyte-like HT-29/B6 cells

The measurement of iron uptake by enterocytes has been described previously and it has been shown that: (i) iron uptake occurs across the AP membrane of enterocytes; (ii) transepithelial flux of iron from AP to basal was low at pH 7.5; and (iii) approximately 96 % of apically applied iron is retained within the enterocytes (Tandy et al., 2000). However, in our study, monitoring of HT-29/B6 transepithelial electrical parameters was started immediately after mounting monolayers into the Ussing chamber. During exposure to 100 μM iron in the apical chamber, 100 ng LPS/ml in the BL chamber and 1 μM oleate in the both AP and BL chambers and measurement of TEER were applied for permeability assessments. As shown in Fig. 2 for *B. pseudolongum*, we found that the TEER values from cultured HT-29/B6 cells in control group remained stable without significant changes in resistance throughout the study. TEER values of *B. pseudolongum* groups remained almost equal for 1 h after incubation. LPS significantly decreased TEER and the TEER levels of LPS group remained the lowest through the 24 h period. Oleate time-dependently decreased TEER. TEER values of iron group decreased slightly over 24 h. However, bifidobacteria significantly inhibited the reduction in TEER induced by treatment with LPS, iron or oleate.

3.3. Bifidobacteria reduced pro-inflammatory cytokines (IL-1β and IL-6) released into the medium in luminal cell milieu of co-cultured cells

We next assessed whether bifidobacteria protected cells by influencing the secretion of inflammatory cytokines. As shown in Fig. 3A and B, stimulation with LPS, excess iron, or oleate resulted in significantly increased secretion of IL-1β and IL-6 as compared with control cells ($p < 0.01$, Fig. 3A and B). However, this stimulated secretion of both inflammatory cytokines was significantly decreased by treatment with bifidobacteria (Fig. 3A and B).

3.4. Bifidobacteria rescued aberrant alteration in the LPS-iron-IL-6-hepcidin axis, reflected in decreased cellular triglycerides and hepcidin in HepG2 cells

We measured the amounts of hepcidin released into the medium in luminal cell milieu of co-cultured cells and of cellular triglycerides levels in HepG2 cells, to verify whether bacteria-secreted factors influenced the biological functions of HepG2 cells. Our results showed that the expression of protein levels of hepcidin in the LPS-, iron- or oleate-treated cells was significantly greater than in the control cells ($p < 0.01$, Fig. 4A). However, treatment with bifidobacteria significantly reduced this increase in hepcidin expression ($p < 0.05$, Fig. 4A). There was a significant positive correlation between high hepcidin and increased pro-inflammatory cytokine levels (IL-6) ($p < 0.001$) (Fig. 3B). These results suggest that bifidobacteria-mediated protection against HepG2 cells-derived elevated hepcidin production may be regulated via IL-6 secretion from HMDMs.

Because any disturbance in the above indicated quaternary receptor signaling complex ultimately leads to impaired cellular lipid metabolism, and because cellular triglyceride levels presumably reflect a complex interplay between substrate (most notably iron) availability, LPS- and/or oleate-mediated triglyceride assembly and excess iron-induced inflammation (Ahemd et al., 2012), we also measured cellular triglycerides. As shown in Fig. 4B, bifidobacteria-mediated inhibition of hepcidin in HepG2 cells is paralleled by reduced cellular triglyceride contents. Relatively similar results were obtained with hepatic Huh7 cells (data not shown).

3.5. Bifidobacteria regulate mRNA expression of key genes whose alteration in the LPS-iron-IL-6-hepcidin axis confers low grade inflammation

To confirm the role of iron-IL-6-hepcidin axis at the intersection of cellular lipid metabolism and inflammatory pathways in response to LPS, iron, or oleate, we investigated the effects of bifidobacteria treatment on the expression of key genes whose alteration in the LPS-iron-IL-6-hepcidin axis confers low grade inflammation. As shown in Fig. 5A–E, our TaqMan qRT-PCR analyses revealed that bifidobacteria downregulated mRNA expression of BMP6 (A), DMT1 (B), TfR1 (C) and TLR4 (D) in enterocytes (here polarized HT-29/B6 cells) following exposure to excessive extracellular LPS, oleate and iron. However, the patterns of ferroportin and TLR2 mRNA expression (C and E) were quite the opposite to those of TLR4 and above indicated genes. Our findings are in agreement with previous studies (Drakesmith et al., 2015, Review) by showing that LPS/TLR4-induced inflammation decreases the expression of ferroportin.

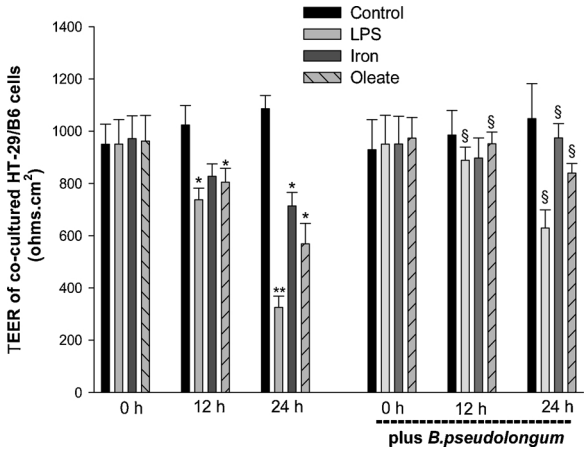

Fig. 2. Effect of LPS, excess iron and oleate on the barrier integrity of intestinal epithelial cells in traditional triple co-culture system consisting of intestinal enterocytes, macrophages and hepatocytes. Bifidobacteria were added to the apical compartment in the presence of 100 μM iron in the apical chamber, 100 ng LPS/ml in the basolateral chamber, and 1 μM oleate, respectively, in both apical and basolateral chambers. Incubation was for up to 24 h. Averages and standard error of the mean (SEM) of 3–5 experiments run in duplicate are shown. Asterisks (*) and (**) indicates significant level versus control $p < 0.05$. The symbol (§) indicates $p < 0.05$ between basolateral LPS alone and basolateral LPS plus bifidobacteria; excess iron alone and excess iron plus bifidobacteria, and oleate alone and oleate plus bifidobacteria, respectively.

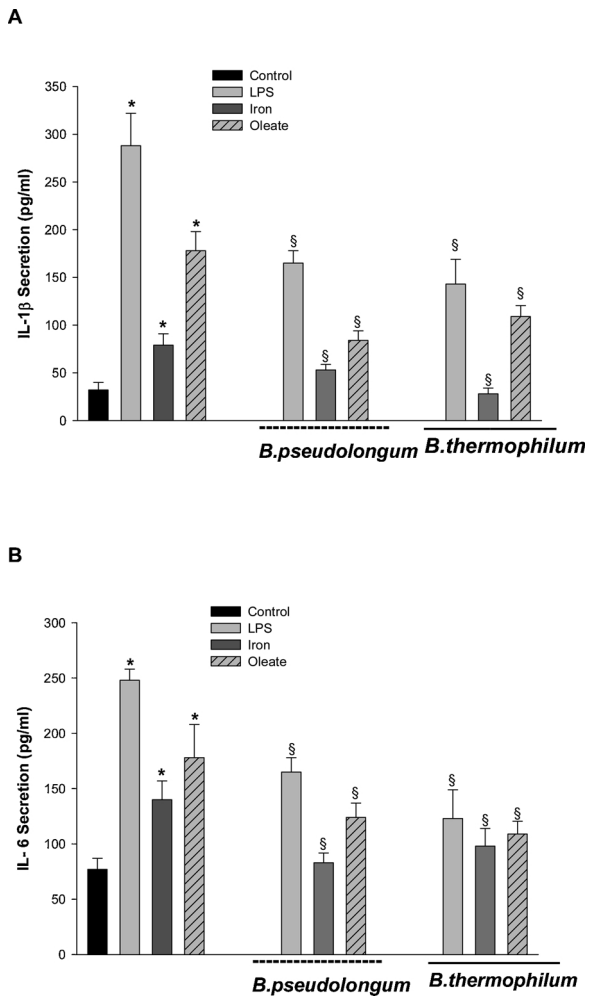

Fig. 3. Effects of bifidobacteria on the secretion of cytokines into the medium in luminal cell milieu of co-cultured cells following exposure to LPS, excess iron, and oleate, respectively. Addition of bifidobacteria was as described in Fig. 2. Incubation was for 24 h. Levels of IL-1β **(A)** and IL-6 **(B)** in the culture supernatants were measured by using ELISA. All data were expressed as the mean ± SEM (n = 4–6). *p < 0.05, vs. the control group; § p < 0.05, vs. the group with LPS alone, group with iron alone, and group with oleate alone, respectively.

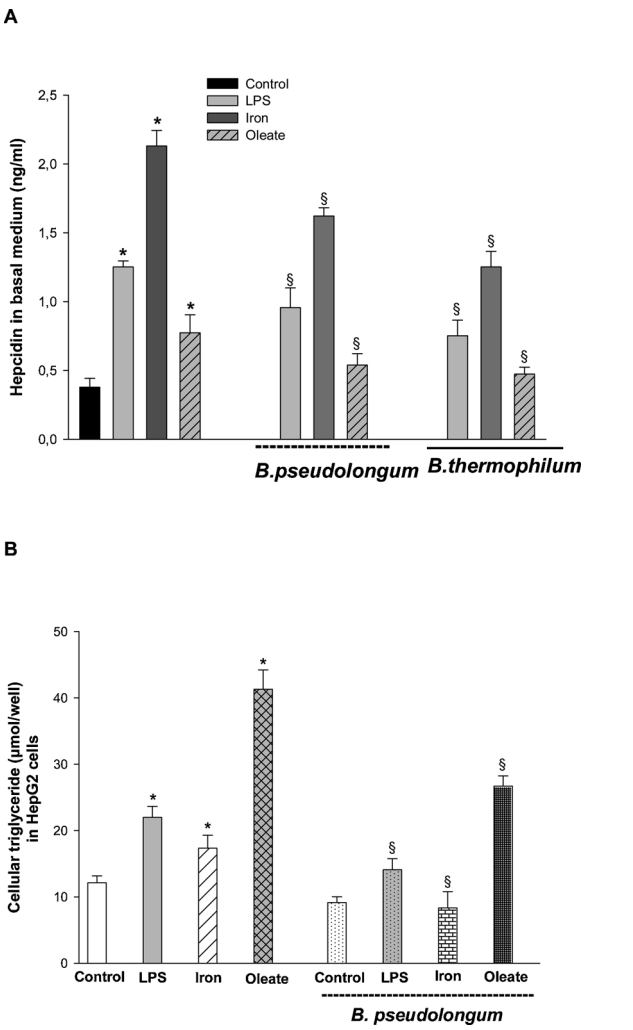

Fig. 4. Bifidobacteria attenuate the protein expression of hepcidin, released into the medium in luminal cell milieu of co-cultured cells, and cellular triglycerides following exposure to LPS, excess iron or oleate. Addition of bifidobacteria was as described in Fig. 2. Incubation was for 24 h. Levels of hepcidin **(A)** and cellular triglycerides **(B)** were detected in culture media and in cell lysates from HepG2 cells, respectively. All data were expressed as the mean ± SEM (n = 4–6). *p < 0.05, vs. the control group; § p < 0.05, vs. the group with LPS alone, group with iron alone, and group with oleate alone, respectively.

3.6. Bifidobacteria regulate mRNA and protein expression of hepcidin inducer IL-6 in HMDMs

To verify whether co-cultured HMDMs - in response to LPS, iron, or oleate - secreted inflammatory markers that affected the HepG2 cells, we assessed both mRNA and protein levels of IL-6 in HMDMs by using qRT-PCR assays and WB, respectively. As shown in Fig. 6A, we observed that after 24-h incubation, bifidobacteria decreased the mRNA expression of IL-6 in HMDMs following exposure of co-cultured cells to LPS, iron citrate, or oleate. Fig. 6B shows a representative WB (upper panel) and the densitometric analysis (lower panel) of IL-6 protein levels, which confirms the decreasing effect of bifidobacteria on expression at the protein level.

3.7. Bifidobacteria regulate mRNA expression of key genes whose alteration in the LPS-iron-IL-6-hepcidin axis confers disrupted cellular lipid metabolism in HepG2 cells

Hepcidin is increased by inflammation as a host defense mechanism to limit extracellular iron availability to microbes (Girelli et al., 2016). We therefore examined the mRNA expression levels of hepcidin, L-ferritin, and STAT3 in HepG2 cells in co-cultured cells.

Our results showed that the expression of mRNA levels of hepcidin in the LPS-, iron, or oleate- treated cells were significantly increased compared to control cells ($p < 0.01$, Fig. 7A). However, treatment with bifidobacteria significantly reduced these increases ($p < 0.05$, Fig. 7A). Furthermore, there was a significant positive correlation between protein (Fig. 4A) and mRNA expression levels of hepcidin in HepG2 cells. Finally, there was a significant positive correlation between high hepcidin levels and increased pro-inflammatory cytokine (IL-6) ($p < 0.001$) (Fig. 3A and B). These results suggest that bifidobacteria-mediated protection against HepG2 cells-derived elevated hepcidin production may be regulated via IL-6 secretion from HMDMs. It is likely, of course, that in our HepG2 cells a post-transcriptional regulation of the ferritin had also occurred, as evidenced by the lack of correlations between ferritin subunit protein and mRNA.

However, downregulated expression results, similar to those reported above, were obtained for ferritin light chain mRNA (Fig. B), and STAT3 (Fig. 7C) in hepatocytes (here HepG2 cells). Our findings agree with previous studies (Torti and Torti, 2002, Review) by showing that LPS elicits a variety of reactions that involve ferritin and TLR4 (Philip

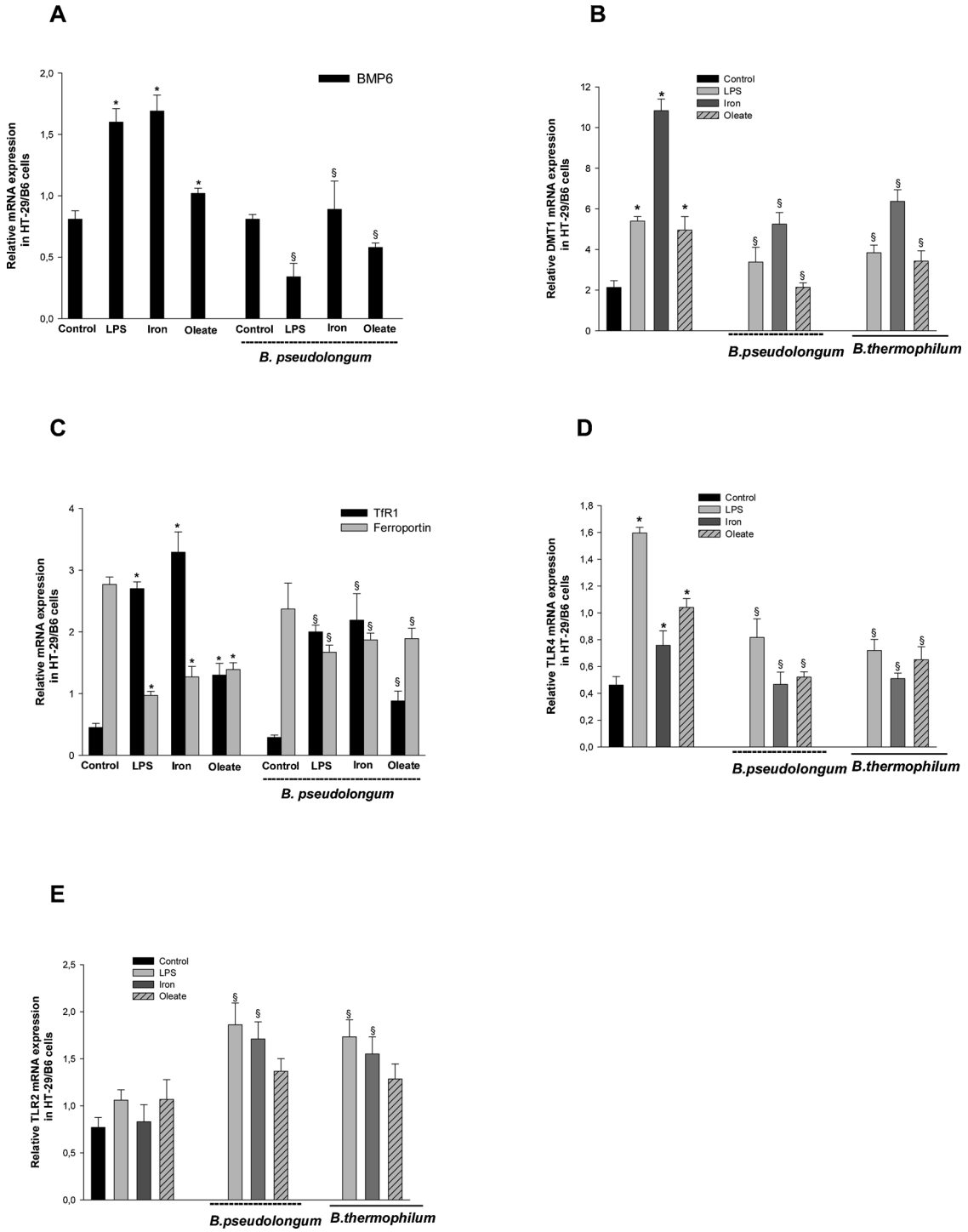

Fig. 5. Influence of bifidobacteria on gene expression responses of triple cell co-culture system following exposure to LPS, excess iron, and oleate, respectively (**A-E**). Addition of bifidobacteria was as described in Fig. 2. Incubation was for 24 h. mRNA levels relative to those of GAPDH were determined by TaqMan RT-PCR. BMP6 (**A**), DMT1 (**B**), ferroportin and TfR1 (**C**), TLR4 (**D**) and TLR2 (*E*) mRNA were first evaluated in HT-29/B6 cells. All data were expressed as the mean ± SEM (n = 4–6). *p < 0.05, vs. the control group; § p < 0.05, vs. the group with LPS alone, group with iron alone, and group with oleate alone, respectively.

et al., 2016) and stimulates the rate of iron oxidation (Roth et al., 2000).

3.8. The bifidobacteria-mediated regulation of BMP6, DMT1, ferroportin, TLR2 and TLR4 mRNA is reflected in protein levels, invoking translational regulation

To validate and correlate the levels of the indicated transcripts (as representative) with those of the proteins, we measured also the levels of BMP6, DMT1, ferroportin, TfR1, TLR2 and TLR4 proteins by WB analysis. As shown in Fig. 8A–F, WB and densitometry analyses showed increased protein levels of BMP6, DMT1, ferroportin, TfR1, and TLR4 in the LPS-, iron-, or oleate-treated cells, compared with the control cells (Fig. 8A, B, C, E and F, respectively). However, treatment with bifidobacteria significantly reduced these increases. Interestingly and similar to the transcriptional profile, the patterns of ferroportin (Fig. 8A, D) and

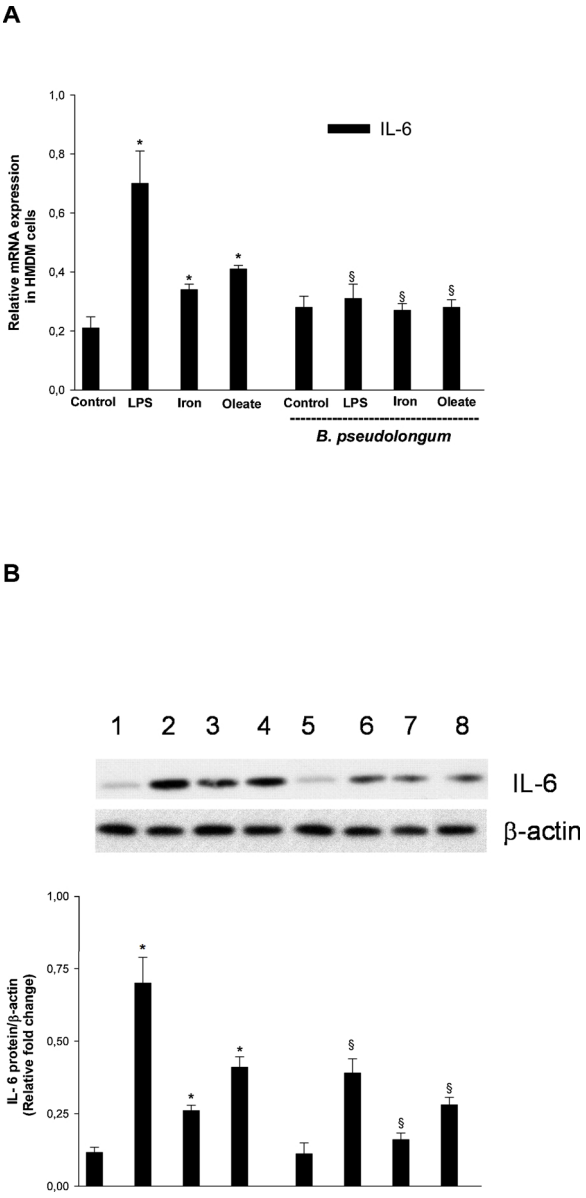

Fig. 6. Influence of bifidobacteria on the mRNA and protein expression of key inflammatory response gene, namely macrophage-derived IL-6, following exposure of triple cell co-culture system to LPS, excess iron, and oleate, respectively. Addition of bifidobacteria was as described in Fig. 2. Incubation was for 24 h. (**A**) Total RNA extraction (from HMDMs), analysis and cDNA conversion were performed as indicated in Material & Methods Section (2.4.1.). mRNA levels of IL-6, relative to those of GAPDH, were assessed using TaqMan RT-PCR. (**B**) Western blot upper panel) and densitometry analysis (lower panel) of hepcidin inducer IL-6 protein in HMDMs. The protein bands were quantitated by densitometry, expressed relative to actin, and normalized to values of untreated control cells. Lane 1, control; lane 2, LPS; lane 3, iron; lane 4, oleate; lane 5, control + *B. pseudolongum*; lane 6, LPS + *B. pseudolongum*; lane 7, iron + *B. pseudolongum*; lane 8, oleate + *B. pseudolongum*. Values plotted are means ± SEMs from at least three independent experiments. *p < 0.05, vs. the control group; § p < 0.05, vs. the group with LPS alone, group with iron alone, and group with oleate alone, respectively.

TLR2 (Fig. 8A and F) protein expression were quite the opposite to those of TLR4.

3.9. The bifidobacteria-mediated regulation of ferritin, hepcidin, TfR1, and STAT3 mRNA is reflected in protein levels, invoking translational regulation

To validate and correlate the levels of the indicated transcripts (as

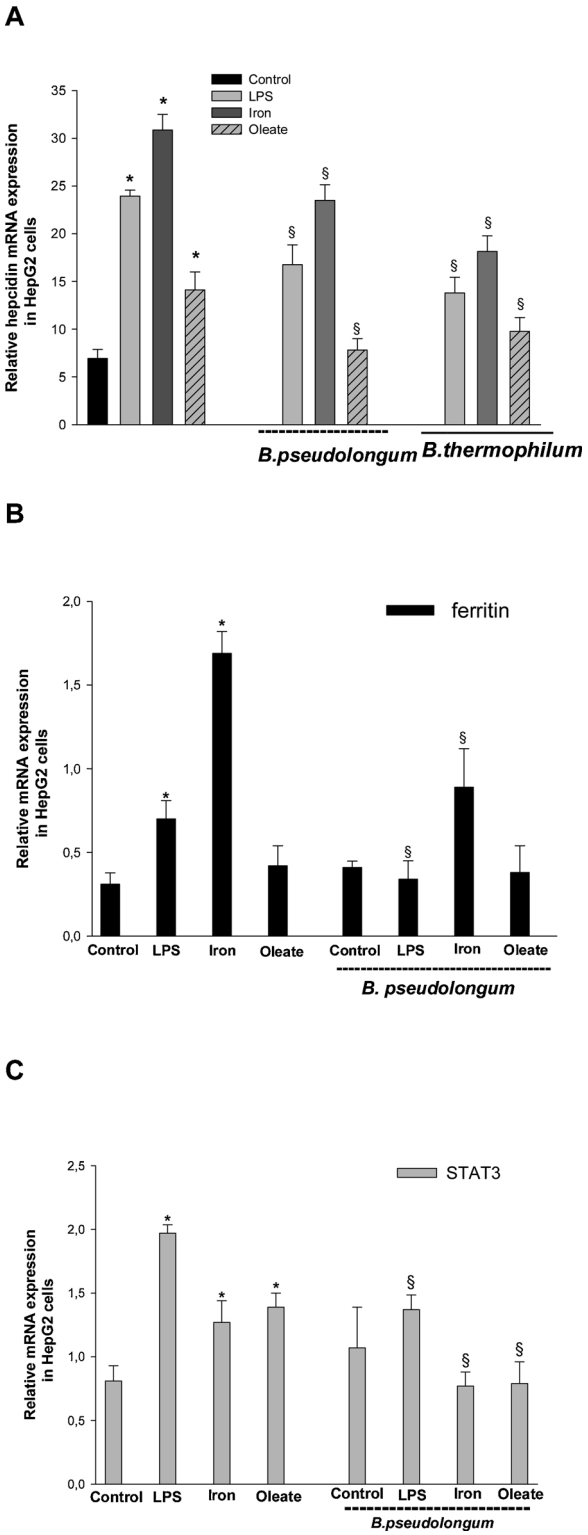

Fig. 7. Influence of bifidobacteria on gene expression of important regulators of links within and across immune response, inflammation, iron hematopoiesis networks following exposure of triple cell co-culture system to LPS, excess iron, and oleate, respectively. Addition of bifidobacteria was as described in Fig. 2. Incubation was for 24 h. mRNA levels of HAMP (**A**), ferritin light chain (**B**), and STAT3 (C) were quantified in HepG2 cells by using TaqMan RT-PCR. All data were expressed as the mean ± SEM (n = 4–6). *p < 0.05, vs. the control group; § p < 0.05, vs. the group with LPS alone, group with iron alone, and group with oleate alone, respectively.

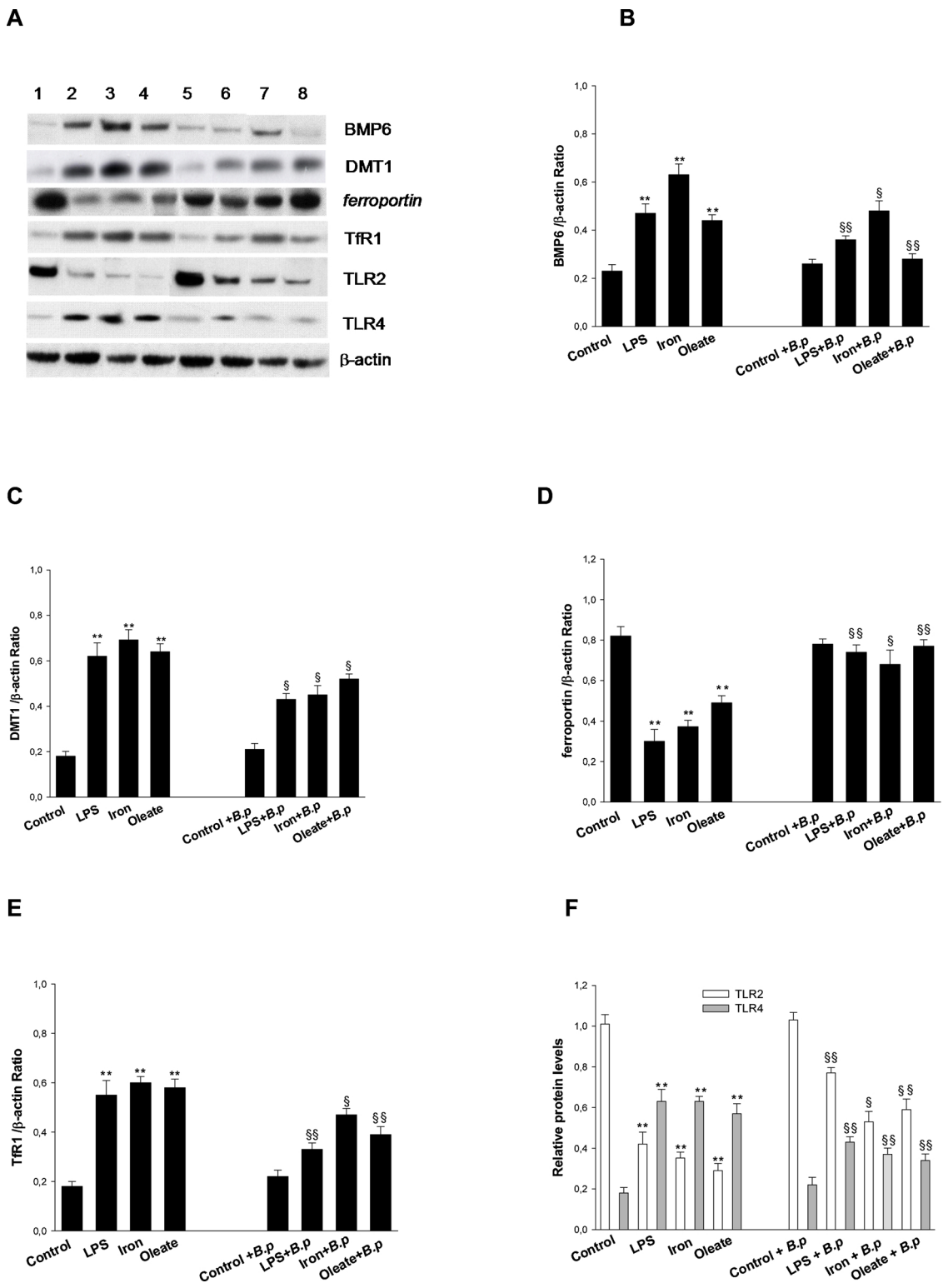

Fig. 8. Western blots (**A**) and densitometry analyses of protein levels of BMP6 (**B**), DMT1 (**C**), ferroportin (**D**), TfR1 (*E*), TLR2 and TLR4 (**F**), respectively, in polarized HT-29/B6 cells following exposure of triple cell co-culture system to LPS, excess iron, and oleate, respectively. Addition of bifidobacteria was as described in Fig. 2. Incubation was for 24 h. Cell extracts were separated by SDS–PAGE. Separated protein bands were analysed by Western blots as described in Materials and Methods. β-actin was used to normalize total proteins. (**A**) Addition of samples to lanes was the same as in Fig. 6. (**B-F**) Densitometry data generated are shown as mean ± SEM of three independent experimentes. $^{*}p < 0.05$, $^{**}p < 0.01$ vs. the corresponding control. $^{\S}p < 0.05$, $^{\S\S}p < 0.01$ vs. no bacteria. *B.p*, *B. pseudolongum*.

representative) with those of the proteins and hepcidin-25 peptide, whole HepG2 cells lysates were subjected to WB for the detection of ferritin, hepcidin-25 peptide, TfR1, and p-STAT3. As shown in Fig. 9A–E, WB and densitometry analysis showed increased protein levels of L-ferritin, hepcidin, and TfR1 proteins in the LPS-, iron or oleate- treated cells, compared with the control cells (Fig. 8A, B, C, E and F, respectively). However, treatment with bifidobacteria significantly reduced the increases in those proteins induced by LPS, iron or oleate. Additionally, LPS-, excess iron-, and oleate-induced phosphorylation of p-STAT3 Ser727 was inhibited by bifidobacteria (Fig. 9A

and E). How bifidobacteria inhibit LPS-, excess iron-, and oleate-induced STAT3 phosphorylation still remains to be determined.

3.10. Modulation effects of bifidobacteria on the LPS/iron/oleate-mediated impaired iron-IL-6-hepcidin signaling axis ultimately leads to mitigated NF-kB activity

To clarify the molecular mechanism of bifidobacteria during LPS-, excess iron-, and oleate-stimulated low grad inflammation, we also assessed transcription factor expression and phosphorylation of various signaling molecules by WB analysis. First, we determined the protein expression levels of NF-κB signaling pathway molecules, including phosphorylated IκBα (p-IκBα), p38 MAPK (p- p38 MAPK) and NF-kB p65 subunit (p-NF-*k*B p65) by using WB. As shown in Fig. 10 A and B, WB and densitometry analysis show significantly increased levels of phosphorylated IκBα (p-IκBα) in HepG2 cells in response to LPS, excess iron, or oleate. In contrast, exposure to *B. pseudolongum* in combination with LPS, iron, or oleate significantly suppressed IκBα phosphorylation.

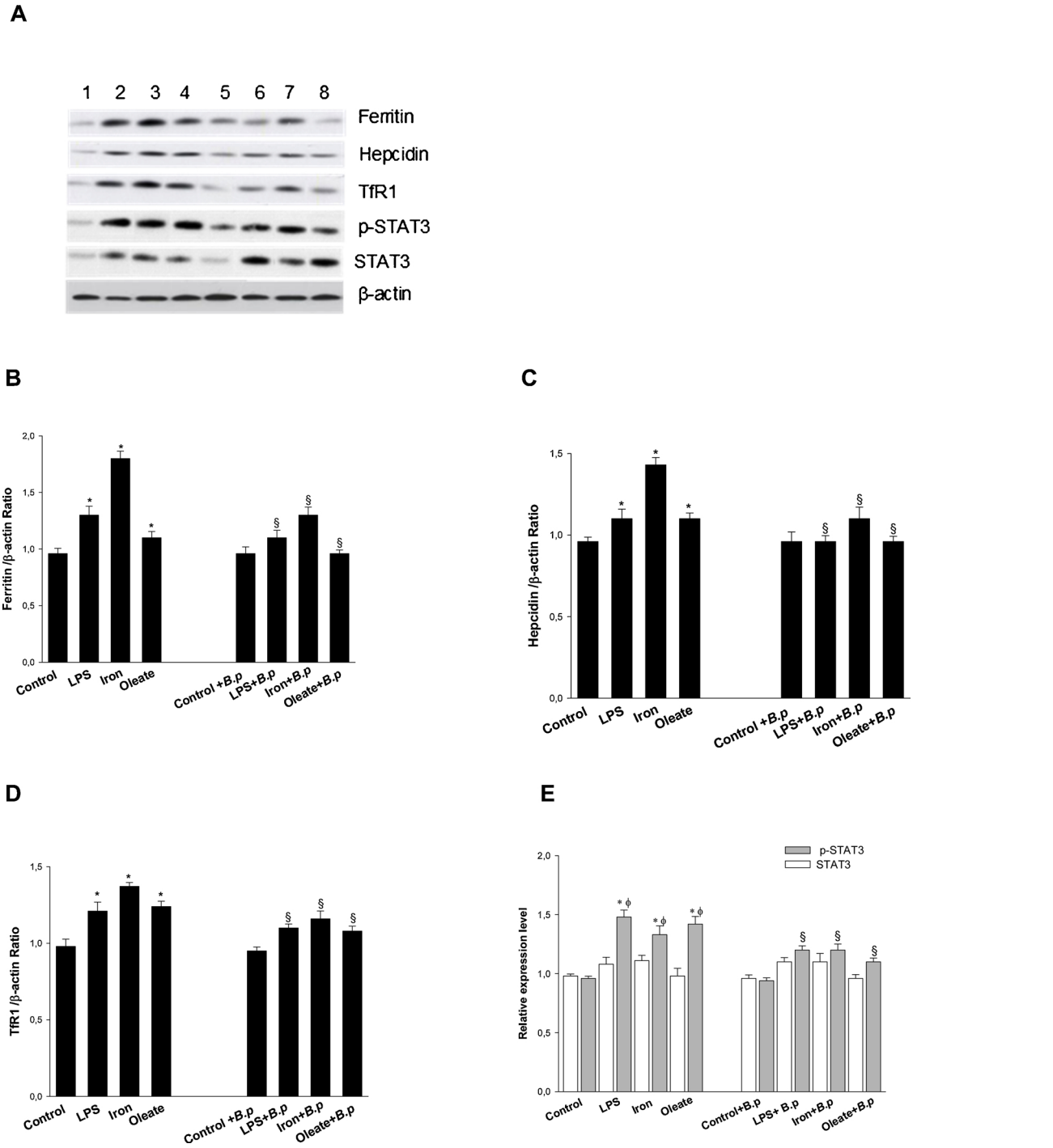

Fig. 9. Western blot (A) and densitometry analysis of protein/peptide levels of ferritin (B), hepcidin (C), TfR1 (D) p-STAT3 and total STAT3 (E), respectively, in HepG2 cells following exposure of triple cell co-culture system to LPS, excess iron, and oleate, respectively. Addition of bifidobacteria was as described in Fig. 2. Incubation was for 24 h. (**A**) Addition of samples to lanes was the same as in Fig. 6. (**B-E**) Densitometry data generated are shown as mean +/− SEM of three independent experimentes. *$p < 0.05$ vs. the corresponding control. $^{\varphi}p < 0.05$ *vs.* the corresponding unphosphorylated STAT3 protein levels. $^{\S}p < 0.05$ vs. no bacteria. *B.p*, *B. pseudolongum*.

Furthermore, we observed a strong induction of phosphorylation (p-NF-kB p65 subunit) after LPS, iron, or oleate treatment, compared with the control cells,which was abolished by *B. pseudolongum* treatment (Fig. 10A and D). The increased phosphorylated NF-*k*B p65 subunit is an indicator of its nuclear translocation and the NF-kB activation state (Ghadimi et al., 2010). On the other hand, the results showed that LPS, iron, or oleate enhanced the expression level of phosphorylated p38 MAPK, while addition of *B. pseudolongum* prevented this

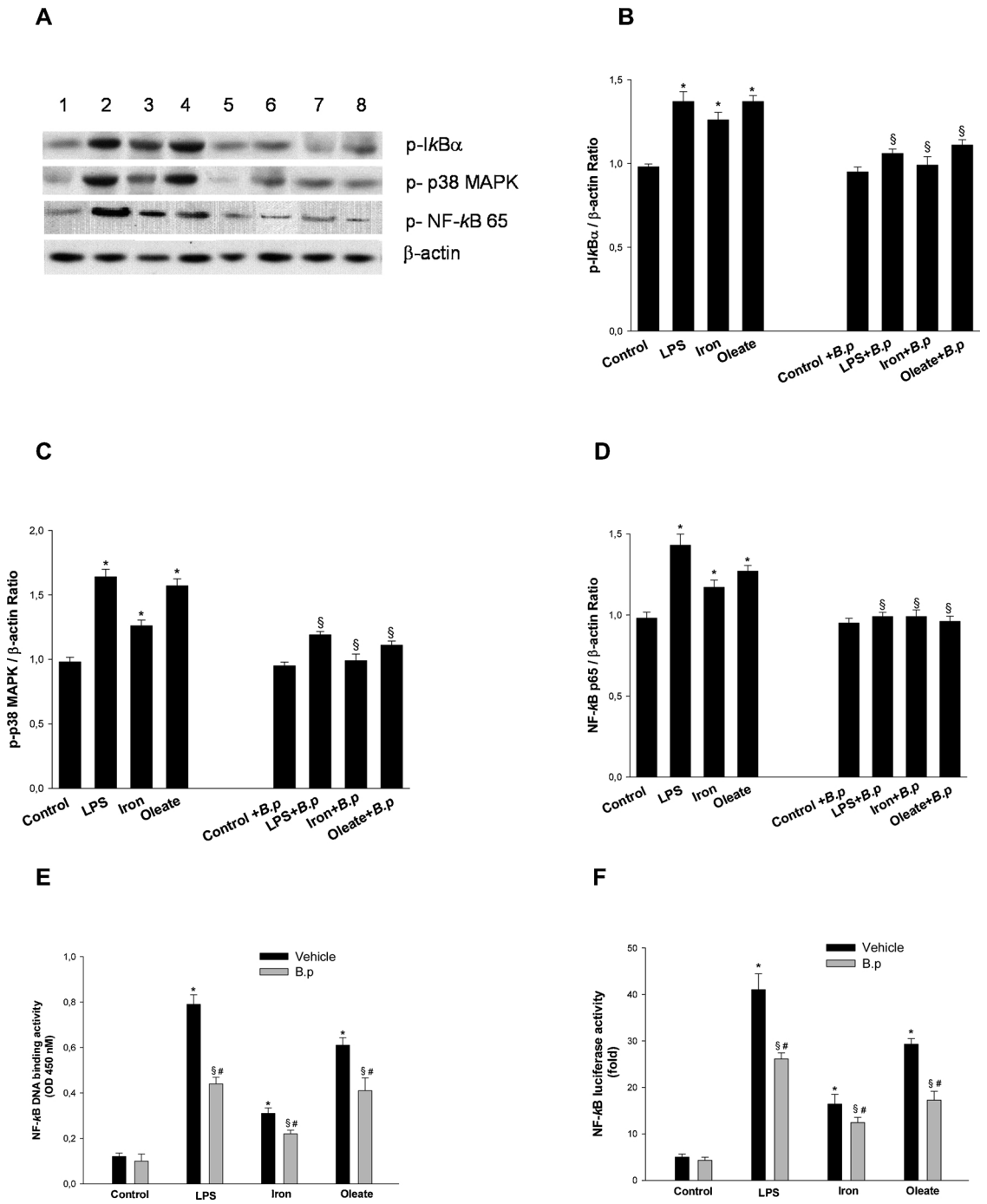

Fig. 10. Bifidobacteria inhibit LPS-, iron-and oleate-induced IkBα phosphorylation/degradation, p38 MAPK phosphorylation and NF-kB transcriptional activity in HepG2 cells co-cultured with HT-29/B6 cells and HMDMs. Western blots (**A**) and densitometry analyses of protein levels of phosphorylated IkBα (p-I*k*Bα) (**B**), phosphorylated p38 MAPK (p-p38 MAPK) (**C**), and phosphorylated NF-kB 65 (p- NF-kB 65) (**D**), respectively, in HepG2 cells following exposure of triple cell co-culture system to LPS, excess iron, and oleate, respectively. Addition of bifidobacteria was as described in Fig. 2. Incubation was for 24 h. (**A**) Addition of samples to lanes was the same as in Fig. 6. (**B-D**) Densitometry data generated are shown as mean ± SEM of three independent experimentes. $^{*}p < 0.05$ vs. the corresponding control. $^{\S}p < 0.05$ vs. no bacteria. (*E*): NF-κB p65 DNA binding activity of nuclear extracts from HepG2 cells was measured using the TransAM NF-κB p65 transcription factor assay kit. (**F**) NF-κB p65 promoter activity measured by luciferase assay. HepG2 cells, transiently co-transfected with Ad5NF-κB-LUC (M of 5) for 12 h, were seeded on the bottom surface of the culture inserts (Transwell) in triple co-culture system and then treated with LPS, iron and oleate, respectively, and bifidobacteria as described in Fig. 2. Incubation was for 24 h. Luciferase activity is expressed as fold increase over control determined as the mean ± SEM of three independent experiments measured in triplicates. $^{*}p < 0.05$ vs. control;.$^{\S}p < 0.05$ indicates the differences in the presence of B.p relative to the medium control group; # $p < 0.05$ vs. Vehicle. *B.p*, *B. pseudolongum*.

phosphorylation (Fig. 10A and C). The ultimate outcome of these effects was, however, reflected in the decline in NF-κB activity. As shown in Fig. 10E and F, *B. pseudolongum* suppressed LPS-, iron-, and oleate-induced overall NF-κB p65 activation (determined by TransAM NF-κB p65 transcription factor assay and NF-κB-dependent promoter luciferase reporter gene assays). As a consequence, the p65-mediated expression of inflammatory genes (Fig. 3A and B) was significantly reduced.

However, to provide mechanistic hints for these effects, we assessed the effects of dead *B.p* and its CFS on expression of key IL-1β, IL-6 and hepcidin. As shown in Fig. 11 A, in LPS-, iron-, and oleate-treated co-cultured cells, we found that IL-1β, IL-6 and hepcidin secretion was lower when co-cultured cells were treated with dead *B.p* or its CFSs. However, secretion and elevation of LPS-, iron-, and oleate-induced cytokines and hepcidin was negligibly decreased by dead *B.p* compared to that of CFS of *B.p* strain. Accordingly, hepcidin expression in co-cultured HepG2 cells stimulated with LPS, with iron, or with oleate was inhibited by both dead *B.p* and its CFS (Fig. 11C and D), suggesting that dead *B.p* and its CFS regulate hepcidin production downstream of pro-inflammatory cytokines. Overall, these results show the importance of bacterial cell-surface structures and metabolites in immunometabolic modulatory axes activities. However, these results showed that killed *B.p* and its CFS exhibited the immunometabolic modulatory effects as well as live *B.p*, but effects of live *B.p* were generally better than those of dead *B.p* and CFS of *B.p*. These differences may be due either to direct contact of *B.p* with enterocytes, utilization/metabolization of iron and oleate, fragmentation of the surface-associated structural components (e.g., PGN, LTA etc.), or all. Therefore, only the effects of live *B.p* have been shown. In addition, note that in Fig. 11(D), an established Gram-negative *E-. coli* strain (K12 TG1) was compared against Gram-positive *B.p* for its ability to inhibit cytokines and hepcidin secretion in a triple co-cultured model representative of the human intestine-liver inter-organ interactions. Our study showed that *E. coli* TG1 did not inhibit LPS-, iron-, or oleate-induced secretion of cytokines and hepcidin. However, its live form synergized with LPS to increase (albeit not

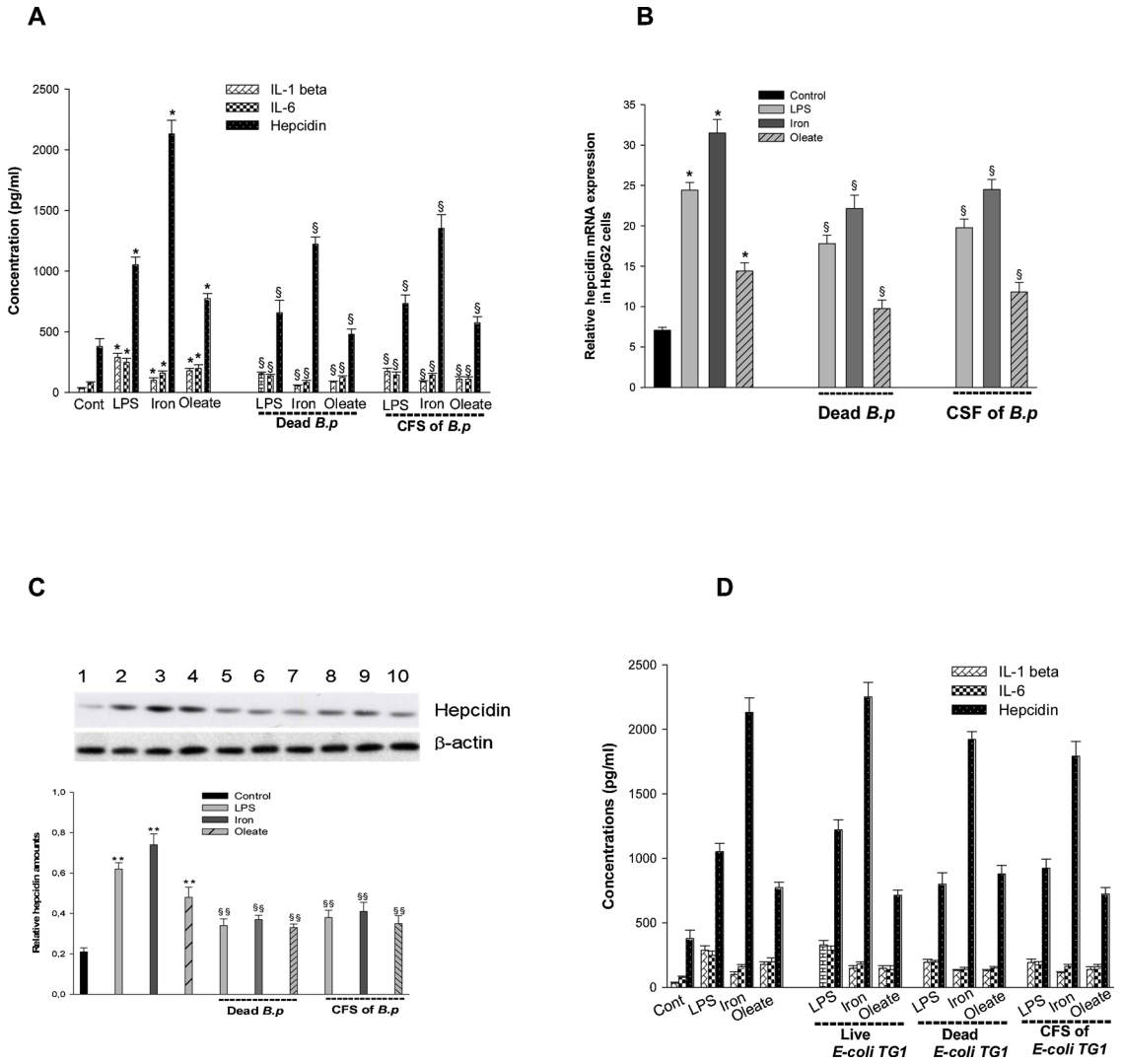

Fig. 11. Patterns of cytokines and hepcidin secretion by Gram-positive *B. pseudolongum* and Gram-negative *E. coli* strain K-12 TG1. **(A)** Immunomodulating effects of heat-killed *B. pseudolongum* and their cell-free supernatants (CFS) on LPS-, iron-, and oleate-induced, IL-1β, IL-6, and hepcidin levels in the culture medium of co-cultured cells. **(B)** TaqMan RT-PCR analysis of relative hepcidin mRNA in co-cultured HepG2 cells in the co-culture system. **(C)** Representative immunoblot analysis of hepcidin and β-actin in co-cultured HepG2 cells in the co-culture system (upper panel). Lane 1, control; lane 2, LPS; lane 3, iron; lane 4, oleate; lanes 5–7, LPS, iron and oleate, respectively, with dead *B. pseudolongugum*; lanes 8–10, LPS, iron and oleate, respectively, with CFS. Intensity of hepcidin bands were normalized to β-actin bands to account for apparent differences and confirm statistical significance. In addition, note that in Figure (D), an established Gram-negative *E. coli* strain (K12 TG1) was compared against Gram-positive B.p for its ability to inhibit cytokines and hepcidin secretion in a triple co-cultured model representative of the human intestine-liver inter-organ interactions; in which, responses were contrasted against those induced by *E. coli* K12 TG1.Values are mean ± SEM of three independent experiments. $^{*}p < 0.05$, $^{**}p < 0.01$ vs. the corresponding control. $^{\S}p < 0.05$, $^{\S\S}p < 0.01$ vs. no dead *B.p* and its CFS. *B.p*, *B. pseudolongum*.

statistically significant) secretion of these markers. However, future trials are planned to test if pathogenic bacteria can be injurious or unfit in this model.

How bifidobacteria, their soluble factors or CFSs inhibit LPS-, iron-, and oleate-induced NF-kB activity and the precise characterization of the active molecules and their mechanism of actions still remain to be determined exactly. It has been suggested that bifidobacteria-mediated inhibition of the NF-κB activity is due to a biologically active compound with proteinaceous nature, which is stable under a variety of temperature and pH conditions (Wang et al., 2011).

4. Discussion

There is evidence that bifidobacteria can internalize and utilize iron. Efficient competition for iron is a key factor for bacterial growth, persistence and establishment in the intestine (Ahmed et al., 2012; Zhu et al., 2015). Despite these evidences, the precise molecular basis and biochemical causes are, however, not well understood.

We observed that bifidobacteria attenuated LPS-, iron-, or oleate-induced secretion of IL-1β and IL-6 into the medium in luminal cell milieu of co-cultured cells (Fig. 3A and B). Among these, IL-6 is a key soluble mediator with a pleiotropic effect on metaflammation (Tolusso et al., 2018), lipid metabolism (Kern et al., 2018), and immune response (Tanaka et al., 2014).

In the real living body, enterocytes, macrophages and hepatocytes are integrated via local and systemic signaling pathways. Macrophages play a pivotal role in iron homeostasis through recycling of host iron-containing compounds (Cassat and Skaar, 2013). Both IL-6 and hepcidin are crucial signaling molecules between macrophages and hepatocytes and key regulators of a variety of processes including iron/lipid metabolism and response to bacterial components (Auguet et al., 2017; Ganz and Nemeth, 2012). Hepcidin transcription is prominently increased by inflammation, predominantly through the activity of IL-6, its receptor and its canonical JAK-STAT3 pathway (Ganz and Nemeth, 2012). Therefore, we explored both the transcriptional and translational levels of IL-6 in co-cultured HMDMs. We found that, concomitant with decreases in IL-6 protein secretion, bifidobacteria inhibited IL-6 transcription/ translation (determined by qRT-PCR and WB) (Fig. 6A and B).

In order to know whether the effect of bifidobacteria on macrophages-derived IL-6 is also intersectionally signalized to the co-cultured HepG2 cells, and to unravel the role of bifidobacteria on macrophages-hepatocytes interplay in the context of cytokine/hepcidin networking, we evaluated transcription and translation levels of hepcidin in HepG2 cells. Our TaqMan qRT-PCR and WB analysis revealed that, concomitant with decreases in hepcidin protein secretion (Fig. 4A), bifidobacteria downregulated mRNA and protein expression of hepcidin following exposure to excessive extracellular LPS, oleate, and iron. Similar results were observed for the other genes, namely ferritin light chain, STAT3 and in HepG2 cells (Figs. 7A–C and 9 A and E). These results suggest that components of the tested bifidobacteria indirectly influence hepatocytes (here HepG2 cells), thus attenuating upstream signal transduction of IL-6-dependent induction of hepcidin production by preventing secretion of the hepcidin inducer IL-6 from macrophages (here HMDMs).

At the first cellular and molecular level and at the area where iron absorption takes place, we observed that applied bifidobacteria could significantly repress mRNA and protein expression of BMP6, DMT1, TfR1 and TLR4 in enterocytes (here HT-29/B6 cells) following exposure to LPS or iron (Figs. 5 and 8). The genes affected are key iron/LPS–signal regulatory genes whose experimental loss or gain-of-function results in significant disruption of cellular iron and lipid metabolism (Ahmed et al., 2012; Auguet et al., 2017; Kell and Pretorius, 2015; Li and Frei, 2009; Yilmaz and Li, 2018).

Because NF-kB, p8 MAPK, and JAK-STAT signaling pathways and their combined tertiary structure determines critical aspects of transcription factor activity in the cellular iron/lipid metabolism and the inflammatory response following exposure to excess iron and bacterial stimuli (Aravindhan and Madhumitha, 2016; Chen et al., 2017; Li et al., 2018; McNelis and Olefsky, 2014), we next assessed NF-κB signaling pathway molecules and overall NF-κB activity. For this, we preferably focused on co-cultured hepatocyte-like HepG2 cells, because the liver is the ultimate and indirect target of circulating gut bacteria-derived signaling molecules or components. Further, it has been shown that increased iron uptake from the GI tract leads to increased iron uptake into and impaired iron release from the liver, which ultimately causes excessive iron accumulation in the liver (Hoki et al., 2015). As shown in Fig. 10A–E, we found that bifidobacteria attenuated the LPS-, iron-, and oleate-enhanced phosphorylation of IκB-α, p38 MAPK and NF-kB p65 subunit in HepG2 cells. As a consequence, overall NF-κB p65 activation and p65 mediated expression of inflammatory genes were significantly reduced (Figs. 3 and 6). The increased phosphorylated IκBα and nuclear NF-κB p65 protein level are indicators of the increased NF-κB activity (Ghadimia et al., 2018). In these experiments, accuracy and reproducibility of quantitative WB analysis was improved using densitometry analysis of WB. Similar effects were observed for phosphorylation of STAT3 when cells were treated with bifidobacteria. The ultimate outcome of these effects, was, however, reflected in the decline in hepcidin production by HepG2 cells (Fig. 4A) as well as cellular in triglyceride contents of HepG2 cells (Fig. 4B).

To validate our results described above and further confirm that bifidobacteria-mediated regulation of LPS/iron/oleate–IL-6/STAT-TLR4/NF-kB-p8 MAPK quaternary signaling pathway ultimately led to the decline of cellular triglyceride contents as an early predictive marker for metaflammation, we measured also cellular triglyceride contents in HepG2 cells. We observed that the addition of bifidobacteria declined LPS-, and oleate-induced cellular triglycerides contents in HepG2 cells. This implies that - although the bifidobacteria, which were added to the AP chamber had no direct interaction with hepatocytes - their MAMPs indirectly and via upstream signal transduction of cytokines (IL-1β and IL-6) production affected the cellular lipid metabolism.

Previous studies, along with ours, explain plausibly how bifidobacteria may affect the NF-kB-p8 MAPK-STAT tertiary signaling complex pathway-mediated lipid synthesis in hepatic cells under *in vivo* milieu. Under inflammatory conditions *in vivo*, LPS, excess extracellular iron, and high-fat diet increase the proportion of LPS-containing gut bacteria and increase intestinal permeability. This leads to elevated circulating endotoxin concentrations and induced inflammatory biomarkers in the intestine and other tissues and organs. Increased circulating levels of LPS triggers TLR4/NF-kB signalling, which is accompanied by aberrant activation of IL-6-hepcidin axis and lipid/iron metabolism master genes BMP6, DMT1, hepcidin, ferritin, IL-6, TfR1, T STAT3 and TLR4 (Calzolari et al., 2010; Jaeggi et al., 2015; Okada et al., 2009; Paganini and Zimmermann, 2017; Schmidt, 2015; Zhang et al., 2017). The exact role and the molecular consequences of these alterations are i) inflammation-induced activation of the IL-6-hepcidin axis, which disrupts iron absorption and iron recycling and storage in related sites, namely in enterocytes, macrophages, and hepatocytes, respectively, and ii) increased expression of pro-inflammatory genes, which strongly correlate with insulin resistance, weight gain, adiposity, plasma insulin and glucose, impaired normal cellular lipid metabolism etc. as hallmarks of metabolic syndrome and metaflammation (Ahmed et al., 2012; Aravindhan and Madhumitha, 2016; Dongiovanni et al., 2015; Ghadimia et al., 2018, 2019; Kell and Pretorius, 2015; Li and Frei, 2009; Meli et al., 2013).

Therefore, the proposed mechanisms and biological molecules, by which bifidobacteria, exert their multitude of effects, is a membrane-based signal from the bacteria or secreted factors (Deschemin et al., 2016; Ghadimia et al., 2018 and 2019). However, it has been shown that lactic acid bacteria and bifidobacteria are capable of utilizing/ metabolizing iron and oleate, making them unavailable to enterocytes and harmful microorganisms (Bezkorovainy et al., 1996; Kishino et al.,

2013; Kot et al., 1995; Paganini and Zimmermann, 2017; Vazquez-Gutierrez et al., 2015). They effectually prevent gut inflammation associated with high-fat-diet, endotoxin, or excess iron (Cani et al., 2007; Okada et al., 2009; Paganini and Zimmermann, 2017; van den Munckhof et al., 2018).

In general, growth of bacterial cells is faster than that of mammalian cells (Ghadimi et al., 2019). To exclude unintended effects, to keep reproducibility, and to get reliable/authentic results in experiments where living bacteria were co-cultured with human tissue in the culture system, a subset of separate experiments was also conducted with dead *B. pseudolongum*. The culture supernatant including secreted metabolic components from *B. pseudolongum* decreased protein levels of pro-inflammatory cytokines (Fig. 11A–D), suggesting that bio-active metabolites or other soluble substances of bifidobacteria are associated with reduced key markers of inflammation.

Together, a schematic diagram showing how commensal bifidobacteria impact on iron/cellular lipid metabolism under inflammatory conditions and on interactions among key biological molecules, which have been studied in this study, is shown in Fig. 12. Bacterial products (e.g.,LPS), excess iron, and dietary fatty acids impact via TLR4 on iron/cellular metabolic/inflammatory pathways through the NF-κB, IL-6/STAT3 and p38 MAPK tertiary signaling complex pathways, which is a nexus for iron/lipid metabolism and cellular signaling (Arndt et al., 2010; Verga Falzacappa et al., 2007). LPS-, excess iron-, and oleate-treatment activates the NF-κB pathway by phosphorylation (p) of NF-κB p65 protein, subsequent nuclear localization, and IκBα degradation (Ub, ubiquitin). Once in the nucleus, phosphorylated NF-κB dimers bind to the promoters of IL-6, IL-1β, and hepcidin and induse gene transcription. IL-6 and IL-1β mRNA are translated into protein and secreted into the medium. Hepcidin mRNA is also translated into protein and acts as a positive regulator of IL-6/STAT3, provoking STAT3 activation and metaflammation. However, commensal bifidobacteria and their soluble factors modulate this process through simultaneous utilization/metabolization of LPS, iron, and oleate, making them unavailable to enterocytes (Arndt et al., 2010; Bezkorovainy et al., 1996; Kishino et al., 2013; Kot et al., 1995; Paganini and Zimmermann, 2017; Philip et al., 2016; Vazquez-Gutierrez et al., 2015) and inhibiting IκBα degradation (Ghadimi et al., 2019). Black lines signify activating connections, whereas red lines signify inhibitory inputs between key regulatory biological molecules.

Considering the functional similarities between the *in vivo* milieu and our *in vitro* model, our experiments may be evidently regarded somewhat artificial. Based on the limitations of this *in vitro* model, extrapolations to *in vivo* effects must be considered with caution. Evidently further *in vivo/in vitro* studies are required to understand the precise mechanisms and to elucidate whether this modulation might be useful in the alleviation of intestinal inflammation and metabolic diseases. In any case, the findings presented here i) support suggestions that pharmacological and/or nutritional strategies aiming at suppressing various steps of endotoxin/ excess iron/high fat diet-triggered inflammation by reducing intestinal-barrier permeability, cellular metabolism pathways (TLR4/NF-kB-p8 MAPK–IL-6/STAT), and expression

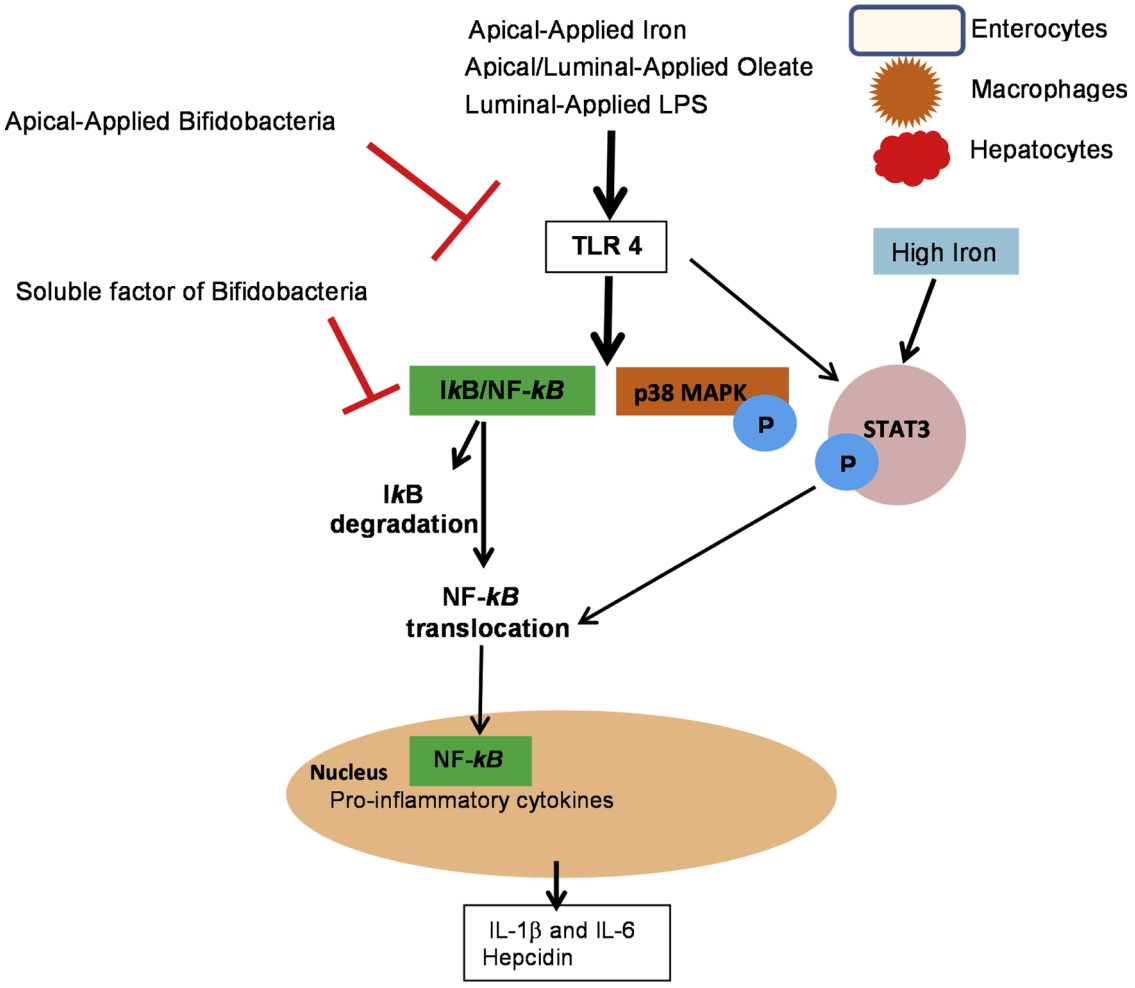

Fig. 12. Schematic diagram showing how commensal bifidobacteria and their soluble factors regulate the molecules and signal transduction pathways involved in cellular iron/lipid metabolism under inflammatory conditions and how key regulatory biological molecules studied in this study interact with each other. See text for further information.

of LPS/lipid/ iron metabolism master genes (BMP6, DMT1, hepcidin, L-ferritin, IL-6, TfR1, STAT3 and TLR4) may be beneficial in both excess iron and high fat diet/endotoxin-associated metaflammation (Ghadimi et al., 2019; Gregor and Hotamisligil, 2011; Kell and Pretorius, 2015; Marmur et al., 2018; Means, 2013; Torti and Torti, 2002); and ii) may explain the molecular and biochemical basis by which commensal bifidobacteria participate in the homeostatic regulation of iron and metabolic processes and by which they improve metabolic diseases-related biomarkers in excess iron and caloric consumption situations like high fat diet-induced inflammation *in vivo* (Dongiovanni et al., 2015; Ghadimi et al., 2019; Meli et al., 2013). This is caused on one hand, by inhibition of TLR4/NF-kB-p8 MAPK–IL-6/STAT tertiary signalling complex pathway, hepcidin production, cellular triglyceride synthesis, and particularly IL-1β and IL-6 secretion in LPS/iron/oleate-stimulated IECs, HMDMs or hepatic cells. On the other hand, it is caused by up-regulation of the activity of the iron exporter ferroportin and TLR2, which is associated with the suppression of peripheral inflammatory responses, thereby preventing leukocyte accumulation at inflamed sites (McKimmie et al., 2009), and preventing metabolic impairments due to excess free fatty acids, HFD (Meli et al., 2013; Dongiovanni et al., 2015; Wan et al., 2014), and complements the *in vitro* and *in vivo* observations of anti-inflammatory and antidiabetic effects of the commensal bifidobacteria (Cani et al., 2007; Yilmaz and Li, 2018).

All in all, we have described a new regulatory mechanism whereby commensal bifidobacteria prevent LPS-, excess iron-, and oleate-associated metaflammation by reducing activity of NF-kB/p38 MAPK/STAT3 pathways leading to reduction of pro-inflammatory cytokines and hepcidin while enhancing ferroportin and TLR2 pathway activity, resulting in normal cellular iron/lipid metabolism. Hence, modulation of NF-kB/p38 MAPK/IL-6/hepcidin/STAT3 cascade by commensal bifidobateria plays an important role for the inhibition of metaflammation-related biomarkers in response to LPS or excess available iron.

Authors statements

All persons who meet authorship criteria are listed as authors, and all authors certify that they have participated sufficiently in the work to take public responsibility for the content, including participation in the concept, design, analysis, writing, or revision of the manuscript. Furthermore, each author certifies that this material or similar material has not been and will not be submitted to or published in any other publication before its appearance in the Immunbiology.

The authors declare that they have no conflicts of interest with the contents of this article. The authors are not part of any associations or commercial relationships that might represent conflicts of interest in the writing of this study (e.g., pharmaceutical stock ownership, consultancy, advisory board membership, relevant patents, or research funding).

Declaration of Competing Interest

The authors declare that they have no conflicts of interest with the contents of this article. The authors are not part of any associations or commercial relationships that might represent conflicts of interest in the writing of this study (e.g., pharmaceutical stock ownership, consultancy, advisory board membership, relevant patents, or research funding).

Acknowledgment

We thank A. Thoss and F. Repenning for helpful technical assistance.

References

Ahmed, U., Latham, P.S., Oates, P.S., 2012. Interactions between hepatic iron and lipid metabolism with possible relevance to steatohepatitis. World J. Gastroenterol. 18, 4651–4658.
Auguet, T., Aragonès, G., Berlanga, A., Martínez, S., Sabench, F., Binetti, J., Aguilar, C., Porras, J.A., Molina, A., Del Castillo, D., Richart, C., 2017. Hepcidin in morbidly obese women with non-alcoholic fatty liver disease. PLoS One 12, e0187065.
Aravindhan, V., Madhumitha, H., 2016. Metainflammation in diabetic coronary artery disease: emerging role of innate and adaptive immune responses. J. Diabetes Res. 2016, 6264149.
Arndt, S., Maegdefrau, U., Dorn, C., Schardt, K., Hellerbrand, C., Bosserhoff, A.K., 2010. Iron-induced expression of bone morphogenic protein 6 in intestinal cells is the main regulator of hepatic hepcidin expression in vivo. Gastroenterology 138, 372–382.
Bailey, J.R., Probert, C.S., Cogan, T.A., 2011. Identification and characterisation of an iron-responsive candidate probiotic. PLoS One 6, e26507.
Bermudez-Brito, M., Muñoz-Quezada, S., Gomez-Llorente, C., Matencio, E., Bernal, M.J., Romero, F., Gil, A., 2013. Cell-free culture supernatant of *bifidobacterium breve* CNCM I-4035 decreases pro-inflammatory cytokines in human endritic cells challenged with *Salmonella typhi* through TLR activation. PLoS One 8 (3), e59370.
Bezkorovainy, A., Kot, E., Miller-Catchpole, R., Haloftis, G., Furmanov, S., 1996. Iron metabolism in bifidobacteria. Int. Dairy J. 6, 905–919.
Briskey, D.R., 2015. The Effects of Multi-strain Probiotics on Liver Disease. Thesis. University of Queensland, School of Medicine, Australia.
Cani, P.D., Neyrinck, A.M., Fava, F., Knauf, C., Burcelin, R.G., Tuohy, K.M., Gibson, G.R., Delzenne, N.M., 2007. Selective increases of bifidobacteria in gut mi.cRoflora improve high-fat-diet-induced diabetes in mice through a mechanism associated with endotoxaemia. Diabetologia 50, 2374–2383.
Calzolari, A., Larocca, L.M., Deaglio, S., Finisguerra, V., Boe, A., Raggi, C., Ricci-Vitani, L., Pierconti, F., Malavasi, F., De Maria, R., Testa, U., Pallini, R., 2010. Transferrin receptor 2 is frequently and highly expressed in glioblastomas. Transl. Oncol. 3 (2), 123–134.
Cassat, J.E., Skaar, E.P., 2013. Iron in infection and immunity. Cell Host Microbe 13, 509–519.
Chen, L., Deng, H., Cui, H., Fang, J., Zuo, Z., Deng, J., Li, Y., Wang, X., Zhao, L., 2017. Inflammatory responses and inflammation-associated diseases in organs. Oncotarget 9, 7204–7218.
Deschemin, J.C., Noordine, M.L., Remot, A., Willemetz, A., Afif, C., Canonne-Hergaux, F., Langella, P., Karim, Z., Vaulont, S., Thomas, M., Nicolas, G., 2016. The microbiota shifts the iron sensing of intestinal cells. FASEB J. 30, 252–261.
Dixit, V.D., 2008. Adipose-immune interactions during obesity and caloric restriction: reciprocal mechanisms regulating immunity and health span. J. Leukoc. Biol. 84, 882–892.
Dongiovanni, P., Lanti, C., Gatti, S., Rametta, R., Recalcati, S., Maggioni, M., Fracanzani, A.L., Riso, P., Cairo, G., Fargion, S., Valenti, L., 2015. High fat diet subverts hepatocellular iron uptake determining dysmetabolic iron overload. PLoS One 10, e0116855.
Drakesmith, H., Nemeth, E., Ganz, T., 2015. Ironing out ferroportin. Cell Metab. 22, 777–787.
Fabersani, E., Abeijon-Mukdsi, M.C., Ross, R., Medina, R., González, S., Gauffin-Cano, P., 2017. Specific strains of lactic acid bacteria differentially modulate the profile of adipokines in vitro. Front. Immunol. 8, 266.
Ganz, T., Nemeth, E., 2012. Hepcidin and iron homeostasis. Biochim. Biophys. Acta 9, 1434–1443.
Ghadimi, D., Hassan, M., Njeru, P.N., de Vrese, M., Geis, A., Shalabi, S.I., Abdel-Razek, S.T., Abdel-Khair, Ael-A., Heller, K.J., Schrezenmeir, J., 2011. Suppression subtractive hybridization identifies bacterial genomic regions that are possibly involved in hBD-2 regulation by enterocytes. Mol. Nutr. Food Res. 10, 1533–1542.
Ghadimia, D., Herrmann, J., de Vrese, M., Heller, K.J., 2018. Commensal lactic acid-producing bacteria affect host cellular lipid metabolism through various cellular metabolic pathways: role of mTOR, FOXO1, and autophagy machinery system. PharmaNutrition 6, 215–235.
Ghadimi, D., de Vrese, M., Heller, K.J., Schrezenmeir, J., 2010. Lactic acid bacteria enhance autophagic ability of mononuclear phagocytes by increasing Th1 autophagy-promoting cytokine (IFN-gamma) and nitric oxide (NO) levels and reducing Th2 autophagy-restraining cytokines (IL-4 and IL-13) in response to Mycobacterium tuberculosis antigen. Int. Immunopharmacol. 10, 694–706.
Ghadimi, D., Fölster-Holst, R., de Vrese, M., Winkler, P., Heller, K.J., Schrezenmeir, J., 2008. Effects of probiotic bacteria and their genomic DNA on TH1/TH2-cytokine production by peripheral blood mononuclear cells (PBMCs) of healthy and allergic subjects. Immunobiology 213, 677–692.
Ghadimi, D., Nielsen, A., Hassan, M.F.Y., Fölster-Holst, R., Michael de Vrese, M., Knut, J.H., 2019. Modulation of GSK - 3β/β - catenin cascade by commensal bifidobateria plays an important role for the inhibition of metaflammation-related biomarkers in response to LPS or non-physiological concentrations of fructose: an in vitro study. PharmaNutrition 8, 100145.
Girelli, D., Nemeth, E., Swinkels, D.W., 2016. Hepcidin in the diagnosis of iron disorders. Blood 127, 2809–2813.
Gregor, M.F., Hotamisligil, G.S., 2011. Inflammatory mechanisms in obesity. Annu. Rev. Immunol. 29, 415–445.
He, W.L., Feng, Y., Li, X.L., Wei, Y.Y., Yang, X.E., 2008. Availability and toxicity of Fe(II) and Fe(III) in Caco-2 cells. J. Zhejiang Univ. Sci. B 9, 707–712.
Hoki, T., Miyanishi, K., Tanaka, S., Takada, K., Kawano, Y., Sakurada, A., Sato, M., Kubo, T., Sato, T., Sato, Y., Takimoto, R., Kobune, M., Kato, J., 2015. Increased duodenal iron absorption through up-regulation of divalent metal transporter 1 from enhancement of iron regulatory protein 1 activity in patients with nonalcoholic steatohepatitis. Hepatology 62, 751–761.
Jaeggi, T., Kortman, G.A., Moretti, D., Chassard, C., Holding, P., Dostal, A., Boekhorst, J., Timmerman, H.M., Swinkels, D.W., Tjalsma, H., Njenga, J., Mwangi, A., Kvalsvig, J.,

Lacroix, C., Zimmermann, M.B., 2015. Iron fortification adversely affects the gut microbiome, increases pathogen abundance and induces intestinal inflammation in Kenyan infants. Gut 64, 731–742.
Kell, D.B., Pretorius, E., 2015. On the translocation of bacteria and their lipopolysaccharides between blood and peripheral locations in chronic, inflammatory diseases: the central roles of LPS and LPS-induced cell death. Integr. Biol. 7, 1339–1377.
Kemna, E., Pickkers, P., Nemeth, E., van der Hoeven, H., Swinkels, D., 2005. Time-course analysis of hepcidin, serum iron, and plasma cytokine levels in humans injected with LPS. Blood 106, 1864–1866.
Kern, L., Mittenbühler, M.J., Vesting, A.J., Ostermann, A.L., Wunderlich, C.M., Wunderlich, F.T., 2018. Obesity-induced TNFα and IL-6 signaling: the missing link between obesity and inflammation-driven liver and colorectal cancers. Cancers (Basel) 11 pii: E24.
Kishino, S., Takeuchi, M., Park, S.B., Hirata, A., Kitamura, N., Kunisawa, J., Kiyono, H., Iwamoto, R., Isobe, Y., Arita, M., Arai, H., Ueda, K., Shima, J., Takahashi, S., Yokozeki, K., Shimizu, S., Ogawa, J., 2013. Polyunsaturated fatty acid saturation by gut lactic acid bacteria affecting host lipid composition. Proc. Natl. Acad. Sci. U. S. A. 110 (44), 17808–17813.
Kitaura, Y., Inoue, K., Kato, N., Matsushita, N., Shimomura, Y., 2015. Enhanced oleate uptake and lipotoxicity associated with laurate. FEBS Open Bio 5, 485–491.
Kot, E., Furmanov, S., Bezkorovainy, A., 1995. Accumulation of iron in lactic acid bacteria and bifidobacteria. J. Food Sci. 60, 547–550.
Li, C., Xu, M.M., Wang, K., Adler, A.J., Vella, A.T., Zhou, B., 2018. Macrophage polarization and meta-inflammation. Transl. Res. 191, 29–44.
Li, L., Frei, B., 2009. Prolonged exposure to LPS increases iron, heme, and p22phox levels and NADPH oxidase activity in human aortic endothelial cells: inhibition by desferrioxamine. Arterioscler. Thromb. Vasc. Biol. 29, 732–738.
Mangin, I., Dossou-Yovo, F., Lévêque, C., Dessoy, M.V., Sawoo, O., Suau, A., Pochart, P., 2018. Oral administration of viable *Bifidobacterium pseudolongum* strain Patronus modified colonic microbiota and increased mucus layer thickness in rat. FEMS Microbiol. Ecol. 94. https://doi.org/10.1093/femsec/fiy177.
Markowiak, P., Śliżewska, K., 2017. Effects of probiotics, prebiotics, and synbiotics on human health. Nutrients 9, 1021.
Marmur, J., Beshara, S., Eggertsen, G., Onelöv, L., Albiin, N., Danielsson, O., Hultcrantz, R., Stål, P., 2018. Hepcidin levels correlate to liver iron content, but not steatohepatitis, in non-alcoholic fatty liver disease. BMC Gastroenterol. 18, 78.
McNelis, J.C., Olefsky, J.M., 2014. Macrophages, immunity, and metabolic disease. Immunity 41, 36–48.
McKimmie, C.S., Moore, M., Fraser, A.R., Jamieson, T., Xu, D., Burt, C., Pitman, N.I., Nibbs, R.J., McInnes, I.B., Liew, F.Y., Graham, G.J., 2009. A TLR2 ligand suppresses inflammation by modulation of chemokine receptors and redirection of leukocyte migration. Blood 113, 4224–4231.
Means Jr, R.T., 2013. Pathophysiology in medicine: hepcidin and iron regulation in health and disease. Am. J. Med. Sci. 345, 57–60.
Meli, R., Mattace Raso, G., Irace, C., Simeoli, R., Di Pascale, A., Paciello, O., Pagano, T.B., Calignano, A., Colonna, A., Santamaria, R., 2013. High fat diet induces liver steatosis and early dysregulation of iron metabolism in rats. PLoS One 8, e66570.
Moen, I.W., Bergholdt, H.K.M., Mandrup-Poulsen, T., Nordestgaard, B.G., Ellervik, C., 2018. Increased plasma ferritin concentration and low-grade inflammation-A mendelian randomization study. Clin. Chem. 64, 374–385.
Mraz, M., Haluzik, M., 2014. The role of adipose tissue immune cells in obesity and low-grade inflammation. J. Endocrinol. 2222, R113–27.
Okada, Y., Tsuzuki, Y., Hokari, R., Komoto, S., Kurihara, C., Kawaguchi, A., Nagao, S., Miura, S., 2009. Anti-inflammatory effects of the genus *Bifidobacterium* on macrophages by modification of phospho-I kappaB and SOCS gene expression. Int. J. Exp. Pathol. 90, 131–140.
Paganini, D., Zimmermann, M.B., 2017. The effects of iron fortification and supplementation on the gut microbiome and diarrhea in infants and children: a review. Am. J. Clin. Nutr. 106, 1688S–1693S.
Philip, M., Chiu, E.Y., Hajjar, A.M., Abkowitz, J.L., 2016. TLR stimulation dynamically regulates heme and iron export gene expression in macrophages. J. Immunol. Res. 2016, 4039038.
Roth, R.I., Panter, S.S., Zegna, A.I., Levin, J., 2000. Bacterial endotoxin (lipopolysaccharide) stimulates the rate of iron oxidation. J. Endotoxin Res. 6, 313–319.
Scheers, N., Sandberg, A.S., 2014. Iron transport through ferroportin is induced by intracellular ascorbate and involves IRP2 and HIF2α. Nutrients 6, 249–260.
Scheers, N., Rossander-Hulthen, L., Torsdottir, I., Sandberg, A.S., 2016. Increased iron bioavailability from lactic-fermented vegetables is likely an effect of promoting the formation of ferric iron (Fe (3+)). Eur. J. Nutr. 55, 373–382.
Schmidt, P.J., 2015. Regulation of iron metabolism by hepcidin under conditions of inflammation. J. Biol. Chem. 290, 18975–18983.
Tandy, S., Williams, M., Leggett, A., Lopez-Jimenez, M., Dedes, M., Ramesh, B., Srai, S.K., Sharp, P., 2000. Nramp2 expression is associated with pH-dependent iron uptake across the apical membrane of human intestinal Caco-2 cells. J. Biol. Chem. 275, 1023–1029.
Tanaka, T., Narazaki, M., Kishimoto, T., 2014. IL-6 in inflammation, immunity, and disease. Cold Spring Harb. Perspect. Biol. 6, a016295.
Tolusso, B., Gigante, M.R., Alivernini, S., Petricca, L., Fedele, A.L., Di Mario, C., Aquilanti, B., Magurano, M.R., Ferraccioli, G., Gremese, E., 2018. Chemerin and PEDF are metaflammation-related biomarkers of disease activity and obesity in rheumatoid arthritis. Front. Med. (Lausanne) 5, 207.
Torti, F.M., Torti, S.V., 2002. Regulation of ferritin genes and protein. Blood 99, 3505–3516.
van den Munckhof, I.C.L., Kurilshikov, A., Ter Horst, R., Riksen, N.P., Joosten, L.A.B., Zhernakova, A., Fu, J., Keating, S.T., Netea, M.G., de Graaf, J., Rutten, J.H.W., 2018. Role of gut microbiota in chronic low-grade inflammation as potential driver for atherosclerotic cardiovascular disease: a systematic review of human studies. Obes. Rev. 19, 1719–1734.
Vazquez-Gutierrez, P., Lacroix, C., Jaeggi, T., Zeder, C., Zimmerman, M.B., Chassard, C., 2015. Bifidobacteria strains isolated from stools of iron deficient infants can efficiently sequester iron. BMC Microbiol. 15, 3.
Vazquez-Gutierrez, P., de Wouters, T., Werder, J., Chassard, C., Lacroix, C., 2016. High iron-sequestrating bifidobacteria inhibit enteropathogen growth and adhesion to intestinal epithelial cells in vitro. Front. Microbiol. 7, 1480 eCollection 2016.
Verga Falzacappa, M.V., Vujic Spasic, M., Kessler, R., Stolte, J., Hentze, M.W., Muckenthaler, M.U., 2007. STAT3 mediates hepatic hepcidin expression and its inflammatory stimulation. Blood 109, 353–358.
Wan, Z., Durrer, C., Mah, D., Simtchouk, S., Little, J.P., 2014. One-week high-fat diet leads to reduced toll-like receptor 2 expression and function in young healthy men. Nutr. Res. 34, 1045–1051.
Wang, Q., Du, F., Qian, Z.M., Ge, X.H., Zhu, L., Yung, W.H., Yang, L., Ke, Y., 2008. Lipopolysaccharide induces a significant increase in expression of iron regulatory hormone hepcidin in the cortex and substantia nigra in rat brain. Endocrinology 149 (8), 3920–3925.
Wang, Z., Wang, J., Cheng, Y., Liu, X., Huang, Y., 2011. Secreted factors from *Bifidobacterium animalis* subsp. *Lactis* inhibit NF-κB-mediated interleukin-8 gene expression in Caco-2 cells. Appl. Environ. Microbiol. 77, 8171–8174.
Williams, H.D., Poole, R.K., 1987. Reduction of iron (III) by Escherichia coli K12: lack of involvement of the respiratory chains. Curr. Microbiol. 15, 319–324.
Yilmaz, B., Li, H., 2018. Gut microbiota and iron: the crucial actors in health and disease. Pharmaceuticals 11, 98.
Zhang, F.L., Hou, H.M., Yin, Z.N., Chang, L., Li, F.M., Chen, Y.J., Ke, Y., Qian, Z.M., 2017. Impairment of hepcidin upregulation by lipopolysaccharide in the interleukin-6 knockout mouse brain. Front. Mol. Neurosci. 10, 367.
Zhu, L., Zhao, Q., Yang, T., Ding, W., Zhao, Y., 2015. Cellular metabolism and macrophage functional polarization. Int. Rev. Immunol. 34, 82–100.